Providing support in relation to the implementation of the EU Soil Thematic Strategy

Potential of Earth Observation for improved soil monitoring

Revision: final document

13-11-2019

Service contract No 07.0201/2016/742739/SER/ENV.D.l

PREPARED FOR:

EUROPEAN COMMISSION
DG ENVIRONMENT

PREPARED BY:

INSTITUTE OF SOIL SCIENCE AND PLANT CULTIVATION –
STATE RESEARCH INSTITUTE

Client European Commission, DG Environment

Title Potential of Earth Observation for improved soil monitoring

Providing support in relation to the implementation of the EU Soil Thematic Strategy is a three-year contract commissioned by the Directorate-General (DG) for Environment (ENV) of the European Commission (Service contract No 07.0201/2016/742739/SER/ENV.D.I, duration 6 Dec 2016 - 5 Dec 2019).

The overall objective is to support DG ENV with technical, scientific and socio-economic aspects of soil protection and sustainable land use, in the context of the implementation of the non-legislative pillars (awareness raising, research, integration) of the Soil Thematic Strategy and the implementation of the European Soil Partnership.

The support includes the production of six in-depth reports providing scientific background on a range of soil and soil-policy related issues in Europe, three policy briefs, logistic and organisational support for six workshops, and the organisation and provision of content to the European website and the wiki platform on soil-related policy instruments.

The work is performed by: Deltares, The Netherlands (coordinator); IUNG Institute of Soil Science and Plant Cultivation, Poland; UFZ- Helmholtz Centre for environmental research Germany; IAMZ - Mediterranean Agronomic Institute of Zaragoza, Spain; CSIC-EEAD Spanish National Research Council - Estación Experimental de Aula Dei, Spain.

Document Information

Title	Potential of Earth Observation for improved land and soil monitoring
Lead Author	Rafał Wawer
Contributors	Grzegorz Siebielec, Artur Łopatka, Soils4EU Partners
Distribution	DG ENV
Report Number	1.8

Disclaimer

Document History

Date	Version	Prepared by	Organisation	Approved by	Review by
19.07.2019	0.1	Rafal Wawer, Artur Lopatka	IUNG-PIB		
09.08.2019	0.2	Rafal Wawer, Artur Lopatka	IUNG-PIB		
13.11.2019	1	Rafal Wawer	IUNG-PIB	Henriette Otter 	Linda Maring 

Table of contents

List of abbreviations

ALEXI	Atmosphere-Land EXchange Inverse
ALTIUS	Atmospheric Limb Tracker for Investigation of the Upcoming Stratosphere
ANC	Areas facing Natural Constraints for agriculture
ASAR	Advanced Synthetic Aperture Radar
ASCAT	Advanced Scatterometer
AVHRR	Advanced Very High Resolution Radiometer
BUFR	Binary Universal Form for the Representation of meteorological data
CCD	Charge-Coupled Devices
COPERNICUS	European Union's Earth Observation Programme
Dis-ALEXI	Disaggregated ALEXI
DOAS	Differential Optical Absorption Spectrometer (SCIAMACHY)
ECMWF H-TESSEL	Hydrology Tiled ECMWF (European Centre for Medium-Range Weather Forecasts) Scheme for Surface Exchanges over Land
EFAS	European Flood Awareness System
ELSUS	European Landslide SUSceptibility map
ENMAP	Environmental Mapping and Analysis Program
ENVISAT	ENVIronment SATellite
EO	Earth Observation
EOEP	Earth Observation Envelope Programme
EOS	NASA Earth Observing System
ESA	European Space Agency
EU	European Union
EUMETSAT	European Organisation for the Exploitation of Meteorological Satellites
EUMETCast	EUMETSAT's dissemination mechanism for the near real-time delivery of satellite data and products
EVI	Enhanced Vegetation Index
GEO	GEO Group on Earth Observations
GEOSS	Global Earth Observation System of Systems
GLDAS	Global Data Assimilation System
GLOSIS	Global Soil Information System
GMECV+	Climate Change Initiative
GMES	Global Monitoring for Environment and Security
GRACE	Gravity Recovery and Climate Experiment
GSC	GMES Space Component
H-SAF	Satellite products for Operational hydrology
Hz	Hertz
InCubed programme	ESA's commercial incubation programme
INSPIRE	Infrastructure for Spatial Information in the European Community
JRC	Joint Research Centre
LAI	Leaf Area Index
LIDAR	LIght Detection And Ranging
LUCAS	Land use and land cover survey
MARS	Multivariate Adaptive Regression Splines

METEOSAT	Meteorological Satellite
MetOp/ASCAT	Advanced Scatterometer form METOP-A satellite
METRIC	Mapping EvapoTranspiration at high Resolution with Internalized Calibration
MLR	Multiple Linear Regression
MSAVI	Modified Soil-adjusted Vegetation Index
MSI (Sentinel)	Multispectral Instrument
MTG	Meteosat Third Generation
MWIR	Mid Wave Infrared Radiation
NDVI	Normalized Difference Vegetation Index
NDSI	Normalized Difference Salinity Index
NDTI	Normalized Difference Temperature Index
NIR	Near Infrared Radiation
NOAA	National Oceanic and Atmospheric Administration
NRT	Near Real Time
OLI (Landsat)	Operational Land Imager
PAR	Photosynthetically Active Radiation
PLSR	Partial Least-Square Regression
Proba-V	PROBA-Vegetation EU satellite
RMS	Root Mean Square error
R/S	Remote Sensing
RUSLE	Revised Universal Soil Loss Equation
S-SEBI	Simplified Surface Energy Balance Index
SAR	Synthetic Aperture Radar
SAVI	Soil-Adjusted Vegetation Index
SCIAMACHY	SCanning Imaging Absorption spectroMeter for Atmospheric CHartographY
SEBS	Surface Energy Balance System
SEBAL	Surface Energy Balance Algorithm for Land
SOM	Soil Organic Matter
SOC	Soil Organic Carbon
SPOT	Satellite Pour l'Observation de la Terre
SWIR	Short Wave Infrared Radiation
SWSI	Crop Water Stress Index
TIR	Thermal Infrared Radiation
TSEB	Two Source Energy Balance
UN	United Nations
UNOSAT	UNITAR's Operational Satellite Applications Programme
USLE	Universal Soil Loss Equation
VIS	Visible Radiation
VNIR	Visible and Near-InfraRed
WDVI	Weighted Difference Vegetation Index
WoSIS	World Soil Information Service

Executive summary

Various satellite platforms are operational, including the recent Sentinel Mission of the European Space Agency (ESA). However, there are still gaps in combining satellite and classical field and laboratory data for improved monitoring of soil quality and degradation. The report provides an overview of remote sensing techniques (chapter 2) and their maturity in assessing the soils' properties and degradation processes.

Remote sensing methods were evaluated in terms of their uptake in soil studies, divided into two main groups:

- Soil properties (chapter 3.1);
- Soil degradation processes (chapter 3.2).

The review of literature and projects from the last 15 years and a Web of Science keyword query for publications issued between 1991 and 2019 indicates that the highest maturity of satellite remote sensing has been achieved in estimating soil moisture and crop residue content where indices are derived directly from reflectance data within chosen satellite spectral bands from scenes with bare soil. Methods are promising but existing Synthetic Aperture Radar (SAR) sensors have too small spatial resolution to be effectively applied in decision support. The limiting factor of direct reflectance interpretation is that soil remains bare in a limited time within the growing season, hence its temporal resolution is limited. Indirect measurement on the other hand base upon indices derived from the condition of crop cover – either thermal or visible and near-infrared (VNIR).

Nine main soil degradation processes were evaluated in terms of how often remote sensing was used as a method of assessing their intensity and spatial extents. The most mature remote sensing methods were used in assessments of soil desertification and sealing as well as flooding and landslide occurrence. Some relatively well-developed methods are used in assessments of soil erosion, especially aerial remote sensing. The least developed methods are in assessing Soil Organic Carbon (SOC) decline and biodiversity as well as salinization. Biodiversity is crucial for sustaining soil health, hence the developments in methodologies for these particular studies are most welcome, similarly for SOC.

The report also elaborates some practical examples (chapter 4), where Earth Observation (EO) and soil information are linked and it ends with a set of recommendations to further improve the use of EO for soil monitoring (chapter 5).

1. Introduction with definitions

There is a wide range of expectations regarding methods of soil remote sensing. The most modest concern the support of classical methods of soil sampling by providing spectral data enabling division of the research area into smaller homogeneous landscape units (segmentation) and limiting the number of samples. Average expectations concern the provision of spatial variables correlated at least locally with soil properties, that can be used to interpolate soil properties into areas between sampling points. The highest demands are made by those, who try to recreate measurements with physical models based on processes in the soil-plant-atmosphere system, combining recorded spectral characteristics with soil properties.

Fast growing numbers of free data from environmental satellite earth observation programs and exponential growth of computing power tempts with the promise of close elimination of time-consuming and expensive soil sampling and analysing. Unfortunately, research so far has been carried out mainly on a local scale (Mulder et al. 2011), and the success of the remote sensing of soil concerns areas / periods without a plant cover. Although proximal sensing methods provide good predictions of soil properties, the transfer of the same procedures to remote sensing still encounters numerous obstacles such as geometric distortions, atmospheric disturbances (clouds, dusts), presence of non-photosynthetic vegetation (crops residues, senescent leafs, woody stems) and lower spectral and spatial resolution resulting in mixing spectral characteristics of soil and vegetation. This means that the increase in temporal, spectral and spatial resolution also increases the possibility of remote sensing of soils and forces periodic assessments of the practical potential of their applications.

This report aims to present the updated state of research in the field and to indicate benefits from linking remote sensing with direct soil measurements.

The most important terms repeatedly used in the report are explained underneath:

Earth observation (EO)[1] – is the gathering of information about the physical, chemical, and biological systems of the planet via remote-sensing technologies, supplemented by Earth-surveying techniques, which encompasses the collection, analysis, and presentation of data.[2]

Remote sensing (R/S)[1] – is the acquisition of information about an object or phenomenon without making physical contact with the object and thus in contrast to on-site observation, especially the Earth. In current usage, the term "remote sensing" generally refers to the use of satellite- or aircraft-based (both manned and unmanned aircraft platforms) sensor technologies to detect and classify objects on earth, including on the surface and in the atmosphere and oceans, based on propagated signals (e.g. electromagnetic radiation)

Proximal sensing[2] – is the measurement of attributes of the soil, vine canopy or fruit, using sensors mounted on vehicles or vineyard machinery operating in the vineyard, i.e. the sensor is operated

[1] http://en.wikipedia.org
[2] Oxford Reference www.oxfordreference.com

close to the target of interest. These sensors are sensitive to different wavelength than multispectral sensors used on satellite platforms and are characterized by high correlation with soil features.

They were developed from a fundamental research using high resolution spectrophotometers on soil samples to choose ranges of wavelength that can be used for detailed close distance soil analyses. One of major research challenges is to copy that high-quality match of spectral response to remote sensing platforms.

Wavelength[3] – In physics, the wavelength is the spatial period of a periodic wave—the distance over which the wave's shape repeats. It is thus the inverse of the spatial frequency.

Band[3] – The electromagnetic spectrum covers electromagnetic waves with frequencies ranging from below one Hertz to above 10^{25} Hertz, corresponding to wavelengths from thousands of kilometres down to a fraction of the size of an atomic nucleus. This frequency range is divided into separate bands, and the electromagnetic waves within each frequency band are called by different names; beginning at the low frequency (long wavelength) end of the spectrum these are: radio waves, microwaves, infrared, visible light, ultraviolet, X-rays, and gamma rays at the high-frequency (short wavelength) end.

Reflectance[3] – of the surface of a material is its effectiveness in reflecting radiant energy. It is the fraction of incident electromagnetic power that is reflected at an interface.

Transmittance[3] –of the surface of a material is its effectiveness in transmitting radiant energy. It is the fraction of incident electromagnetic power that is transmitted through a sample.

Multispectral image[3] is one that captures image data within specific wavelength ranges across the electromagnetic spectrum. The wavelengths may be separated by filters or by the use of instruments that are sensitive to particular wavelengths, including light from frequencies beyond the visible light range, i.e. infrared and ultra-violet. Spectral imaging can allow extraction of additional information the human eye fails to capture with its receptors for red, green and blue. Multispectral imaging measures light in a small number (typically 3 to 15) of spectral bands. Hyperspectral imaging is a special case of spectral imaging where often hundreds of contiguous spectral bands are available.

Absorptance[3] – is the radiation absorption effectiveness i.e. fraction of incident radiation power that is absorbed at a surface and in case of solar radiation converted into heat, evapotranspiration or into chemical energy of photosynthesis products.

Polarization[3] - direction of oscillation of the electric field vector in the electromagnetic wave.

Scattering[3] - change in radiation propagation from directionally ordered to multidirectional. The shorter the waves, the more strongly they are scattered, because the direction of propagation changes on in-homogeneities of the propagation medium with the size of the wavelength range (Mie scattering), slightly smaller in the case of propagation in a polarizable medium (Rayleigh scattering)

[3] http://en.wikipedia.org

or several times larger in case of non-wavelength-selective scattering of visible radiation (VIS) on water droplets in clouds.

2. Overview of remote sensing techniques

The short overview of remote sensing techniques presented here is based on detector types for different wavelength ranges. The selection of the wave range for imaging various soil properties is mainly related to the model of the phenomenon allowing the best reinterpretation of main surface parameters recorded in the pictures: temperature, roughness and height differences. However, it is also necessary to search for remote registration methods that minimize the disturbing effects of the atmosphere, plant cover or limitations of the sensors themselves. The wavelength is also decisive for them in accordance with the general rule that shorter waves interacting with smaller objects allow for more precise surface variability detection, easier, cheaper registration in small, light sensors but also stronger absorption and dissipation when passing through the atmosphere than it is in case of longer waves. Optical and thermal techniques are used both as remote and proximal methods, i.e. using satellites, airplanes, helicopters, drones, balloons and detectors mounted on vehicles. The typical satellite method is gravimetry and the methods used mainly using airplanes (low-level remote sensing) are LIDAR (light detection and ranging), microwave and cosmic ray neutron scattering techniques. Proximal sensing methods are more detailed described in section 2.7.

2.1 Optical techniques

Methods based on optical detectors of visible (VIS), near infrared (NIR), short wave infrared (SWIR) and mid infrared (MWIR) electromagnetic radiation are the oldest and the most widely used satellite remote sensing techniques. In the early EO development period cameras recording images on the photographic film were used for optical wavelength range detection. Currently optical detection is done by radiometers where radiation is focusing by glass lenses, wavelength selected by diffraction gratings or filters and detected by charge-coupled devices (CCD) consisting from arrays of semiconductor pixels. Typical ground sampling distance corresponding to one pixel is about several meters for VIS and from several to 30 meters for infrared radiation (IR). Due to limitations in the transmission speed of recorded images, higher spatial resolutions in the optical range are obtained at the expense of a smaller image area or a lower image registration frequency.

Visible radiation (VIS) with wavelengths from $4 \cdot 10^{-7}$ to $7 \cdot 10^{-7}$ m (400 – 700 nm) is emitted or absorbed by energy level transitions of electrons in atoms and could be observed as atomic line spectra.

VIS propagation through the cloud free atmosphere is little attenuated and limited mainly by the radiation absorption of oxygen and ozone molecules and scattering by aerosols and gases. Presence of clouds and their high reflectance is the main problem for earth and soil observations in the VIS region in the projects requiring observations repetition in a rigid time frame.

Range of VIS radiation is approximately overlapping the range of radiation absorbed by plants called *photosynthetically active radiation* PAR (e.g. Jones, Vaughan 2010). Most of the chlorophyll absorption occurs in red light and in a large part in blue. Carotenoids and xanthophylls (pigments

dominant in the leafs during autumn or in the stress periods and giving them yellow-orange colours) mainly absorb light in the blue-green region.

Soils reflectance in the visible region is linearly and smoothly growing from blue light to red. Soils reflectance decreases in this spectra region with:

- increase in soil moisture (due to absorption in water bands),
- increase in SOC fraction (due to presence of black humic acid and water retention growth (Viscarra Rossel et al. 2006)),
- increase in small particles fractions (clay),
- increase in soil roughness,
- increase in iron oxides (red soils).

Near infrared radiation (NIR) with longer than visible wavelengths from $7 \cdot 10^{-7}$ to $1 \cdot 10^{-6}$ m (700 – 1000 nm) is still short enough to provide atomic line spectra or narrow range wavelength absorptions bands.

Propagation of NIR through atmosphere occurs for the wavelength intervals known as atmospheric windows which are separated by absorption bands of atmospheric gases – mainly CO_2 and H_2O vapour.

NIR bands are commonly used for vegetation detection by many indexes, like Normalized Difference Vegetation Index (NDVI) defined by formula:

$$NDVI = \frac{\rho_{NIR} - \rho_{RED}}{\rho_{NIR} + \rho_{RED}}$$

where: ρ is the reflectance, with subscript letters NIR for near infrared radiation, which is almost entirely reflected from the plant surface and a RED for the visible spectrum radiation, which is strongly absorbed by chlorophyll. Since the function between NDVI and leaf area measured by Leaf Area Index (LAI) for range LAI> 2 is saturated with values from 0.6-0.8, the error for LAI estimation based on NDVI in this range is large (Jones, Vaughan 2010) and in the middle of the growing season, NDVI practically does not differentiate vegetation with high but different LAI. In addition, when the plant cover is rare, the relationship between NDVI and LAI disturbs the reflection from the soil surface. There are indicators in which one of the described problems has been reduced, however NDVI is still the simplest and most frequently used indicator in this type of applications (Jones, Vaughan 2010).

Short wave infrared radiation (SWIR) with wavelengths from $1 \cdot 10^{-6}$ m to $3 \cdot 10^{-6}$ m, and mid infrared radiation (MWIR) with wavelengths from $3 \cdot 10^{-6}$ m to $4 \cdot 10^{-6}$ m, are separated by wide absorption bands of water vapour. Their importance for soil remote sensing is slightly smaller than shorter optical waves.

The summary of spectral bands used in Landsat 7, Landsat 8 and Sentinel-2, compared with atmosphere windows (grey) in the spectrum between 400 and 13000nm are given in figure 1.

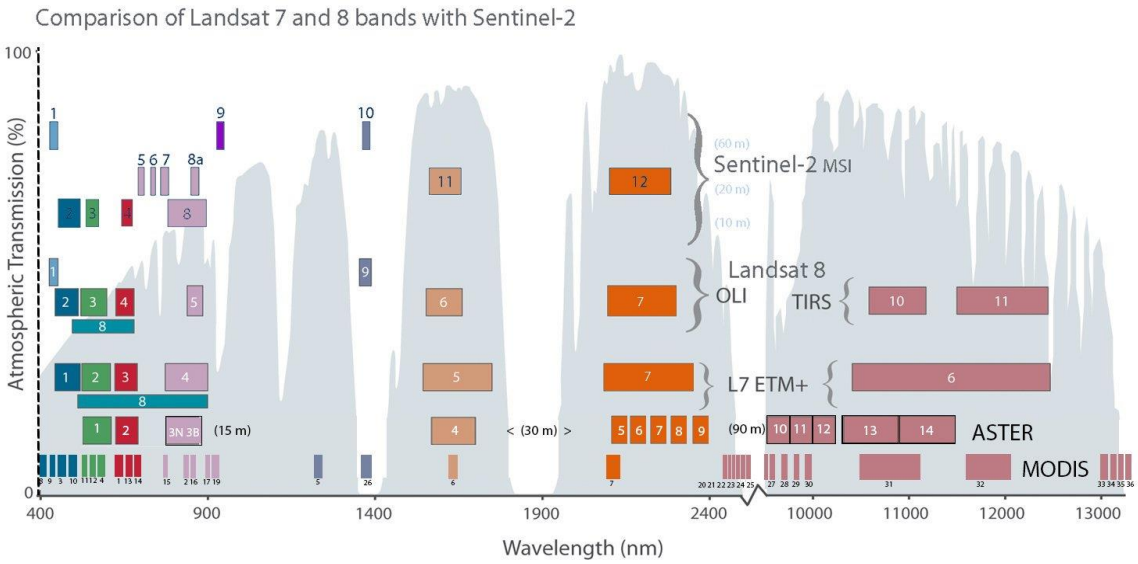

Figure 1. Comparison of LAndsat 7&8 with Sentinel 2 mission

Source: USDA 2016 (https://twitter.com/usgslandsat/status/773939936755982336)

2.2 Thermal techniques

Thermal infrared radiation (TIR) refers to wavelengths from $4 \cdot 10^{-6}$ m to $15 \cdot 10^{-6}$ m and requires different type of detectors than radiation of optical range. Because TIR is less energetic, detection encounters the problem of a lower signal-to-noise ratio and the detectors must be cooled down. Interaction of TIR with atmosphere is dominated by molecular rotations and vibrations resulting in broader absorption bands. Since TIR is emitted by all objects with temperature above absolute zero, it is commonly used for earth surface temperature detection.

2.3 Radar/Microwave techniques

Microwave range radiation, commonly called as radar, refers to wavelengths from $4 \cdot 10^{-3}$ m to 1 m and requires detectors similar to radio antennas registering not only radiation intensity but also their polarization. Due to the longer wave the advantage of radar radiation is the ability to detect through clouds and in case of active systems also at night. This property might be especially valuable in the case of monitoring systems e.g. agricultural drought where uninterrupted observation of humidity conditions is necessary.

2.4 Gamma ray spectrometry

Gamma-ray radiation refers to wavelengths shortest than $5 \cdot 10^{-11}$ m, detected by radiometers installed mainly on aircrafts. Gamma-rays are emitted by radioactive decay of atoms – mainly potassium (^{40}K), thorium (^{232}Th) and uranium (^{238}U) in the top 30cm layer of rock or soil (Read et al. 2017). Because the clay fraction in some regions has higher levels of radioactive atoms, this method can be useful for remote sensing of soil texture. Detection of soil contamination with radioactive products is possible provided that the level of pollution significantly modifies the level of natural radioactivity of soil and rocks. This usually happens after reactor catastrophes and in radioactive waste repositories. Remote sensing of soil contamination with gamma radiation detectors is today possible from the airborne level using both planes (Souza et al. 1997, Connor et all. 2016) and the unmanned aerial vehicles (Martin et al. 2016, Connor et all. 2016).

2.5 Cosmic ray neutron scattering techniques

Fast neutrons emitted by radioactive source are slowed by elastic collisions with atoms nuclei. Most energy is released by neutrons colliding with the nuclei of light elements - in the soil hydrogen atoms from water. Slowed neutrons are counted in detectors and recalculated into water content in the soil. Since cosmic rays are continuously providing highly energetic neutrons, it is possible to detect them after interaction with water. Cosmic ray neutron scattering technique is mainly used for soil moisture monitoring and based on ground detectors, but the detection range is over hundreds of square metres which makes it similar to other remote sensing methods. Thanks to the large reading range, the humidity is averaged and ensuring the representativeness of the measurements does not require an expensive network of sensors as in other terrestrial methods (Vather et al. 2018).

2.6 Gravimetry

Gravimetric remote sensing focuses on measuring the earth's gravitational field and its fluctuations. ESA's GRACE (Gravity Recovery and Climate Experiment) mission, launched in 2002 and ended in 2017, was built as a set of two satellites orbiting the earth and measuring the gravitational field of the earth. There was an example of global gravimetric survey, that was being used to estimate water content on the lands using GRACE. Its resolution of 1 degree can be scaled up within GLDAS program (Global Data Assimilation System) up to 0,25 degree (Badora, 2016). It was not suitable for detailed advisory service however good enough to provide regional and continental balances of water on land. The follow-up mission for GRACE is GRACE-Follow-On, launched in 2018. It may be used in small-scale assessments dealing with large area ground and surface water dynamics as a response to climate, that indirectly affect soils in a long term, shaping the water balance.

2.7 Low altitude spectroscopy with hyperspectral imaging

This is a technique dedicated for on-ground studies of soil properties. It is mentioned here because of its potential for being used to depict empirically new spectral bands for satellite and aerial sensors.

High resolution, hyperspectral spectroscopes are used in studies related to proximal sensing of soil properties. The spectral resolution reaches 5nm and range usually lie within VIS-NIR (350nm-2500nm). The results indicate high predictability of soil features: texture, soil moisture, the nutrients N,P,K, and Soil Organic Matter (SOM), reaching r^2=0,6-0,96 for the latter. The bands optimal for correlating reflectance with soil features are given on the example of SOM in **Error! Reference source not found.**.

Table 1. Review of spectral bands used in SOM estimates (Niedzwiecki and Debaene, 2013)

Spectrum	Spectral range [nm]	RMSE	R2	Authors
VIS	400-950	0,36	0,91	Aicha at al., 2009
VIS-NIR	350-2500	0,79	0,87	Brown et al., 2006
NIR	1100-2500	0,32	0,96	Fidencio et al., 2002
NIR	700-2500	0,18	0,6	Viscarra Rossel et al., 2006
VIS-NIR	400-2200	0,11	0,68	Debaene et al., 2010
VIS-NIR	400-2200	0,12	0,71	Debaene et al., 2014
VIS-NIR	430-2500	0,42	0,94	Wetterlind et al., 2010
NIR	800-2600	1,1	0,71	Moros et al., 2009

MIR	2500-25000	0,84	0,97	Messerschmidt et al., 1999

There are numerous studies correlating spectroscopy with content of particular substances in soil, e.g. heavy metals (Siebielec et al., 2004) – see chapter 3.2.3.

2.8 LIDAR

LIDAR is a surveying method that measures distance to a target by illuminating the target with laser light and measuring the reflected light with a sensor. Differences in laser return times and wavelengths can then be used to make digital 3-D representations of the target. LIDAR installed on airplanes are widely used in mapping of topographic terrain features and land cover. In soil-related research they may be utilized in mapping soil erosion by water, especially rill erosion (e.g. Vinci et al., 2015). LIDARs, mounted on manned or unmanned aircraft vehicles are also used in remote areas for assessing soil typology from topographical features.

3. Evaluation of the potential of these techniques for land and soil monitoring

Based on the literature review, the methods used for remote soil research, their limitations and the quality of predictions in comparison with ground measurements are discussed. An expert assessment of the potential of the methods used for remote observation of soils was carried out, both for the further development in the field of soil science and for the practical needs of farmers or environmental quality monitoring. Cost estimates were made only to the time and complexity of images processing, assuming that the images themselves were free of charge. The state of art was analysed based on scientific papers from the last 15 years (2005-2019) and a keyword search in Web of Science for the period 1991-2019.

The uptake of Earth Observation methods in assessing soil properties has been screened as the level of maturity of the EO methods in literature. Three levels of maturity were distinguished:

1. Direct measurement, where EO methods to assess a given soil property utilize directly reflectance of particular wavelengths. A good example is here the content of crop residues, which directly measures reflectance in the band near 2100nm;
2. Indirect indices, where methods measure reflectance that corresponds to a soil property that is directly correlated with another property that is actually assessed. A good example here may be SOM estimates based upon soil colour and clay content.
3. Modelling inputs from EO, meaning that the property to be measured can be calculated from other soil and non-soil related features using models, which inputs are directly or indirectly measurable by EO methods. Good example here is soil erosion, where there are many models for calculating soil erosion rates and extents, the Revised Universal Soil Loss Equation (RUSLE) being one of most widely used. Most of the RUSLE indices can be derived from EO measurements.

3.1 Potential and maturity of techniques to measure soil properties

In the sections below, the potential for techniques for different soil property are given and the maturity is assessed (3.5.7).

3.1.1 Soil moisture

Soil moisture is crucial from a practical point of view, being a key indicator influencing the requirements for irrigation and crop yields. It also influences soil strength and stability of aggregates as well as the soil capacity to accumulate and maintain organic matter stock. When soil moisture is too low, it makes light soils more susceptible to wind erosion, while if too wet – medium and heavy soils are more susceptible to water erosion (Wawer et al., 2013a,b).

Optical remote sensing methods utilize the solar band with wavelengths between 400nm – 2500nm measuring the solar radiation reflected from the earth's surface. Many investigations indicate the potential of optical methods, but microwave and thermal infrared bands are most often used in soil moisture estimates (Wang and Qu, 2009).

In currently operational on-line information services direct soil moisture for bare soil are being estimated by EUMETSAT (Table 2), that produces level 2 near real time (NRT) surface soil moisture

index using advanced scatterometer (ASCAT) data (Binary Universal Form for the Representation of meteorological data (BUFR) format). The index of soil moisture [%] represents the saturation degree in upper soil layers (up to 5cm). It ranges from 0 (dry) to 100 (saturated). The spatial resolutions of this datasets are 25x25km or 50x50km with a temporal resolution over Europe reaching 1,5 days. The average RMS error of the index measurement for 25x25km resolution dataset varies between 3-7% (volumetric water content) and depends of the soil type.

Another data source for soil moisture index is H-SAF scatterometer based on the MetOp/ASCAT data. Initial 25x25km resolution dataset is being disaggregated and re-sampled to 1km by overlaying it with ENVISAT ASAR dataset. Spatial resolution varies between 1km-25km, while temporal resolution is 1,5 days over Europe with several gaps of coverage. The product (BUFR format) is delivered in NRT on EUMETCast and off-line by EUMETSAT Data Centre.

Table 2. Satellite products for estimation of soil moisture from EUMETSAF mission.

Satellite product	Horizontal resolution	Temporal resolution	Data availability delay	Condition of observation	Terms of use
Soil moisture index ASCAT	25 km	Full coverage over Europe in 36 h	NRT	land	License
EUMETSAT H-SAF Soil moisture index ASCAT+ASAR	1 km	36 h	NRT	land	License

Several on-line services were built on top of ASCAT data, e.g. Polish Institute of Meteorology and Water Management[4]. The service bases upon EUMETSAT H-SAF and utilizes ECMWF H-TESSEL Land Surface Model (Hydrology Tiled ECMWF Scheme for Surface Exchanges over Land) for the estimation of soil moisture content in the soil profile down to 7-28 cm in 10-30cm layers. The way the service presents data makes it usable only for very rough overview of the soil moisture situation while the values are discussable (**Error! Reference source not found.**2).

[4] http://agrometeo.pogodynka.pl/obrazysat

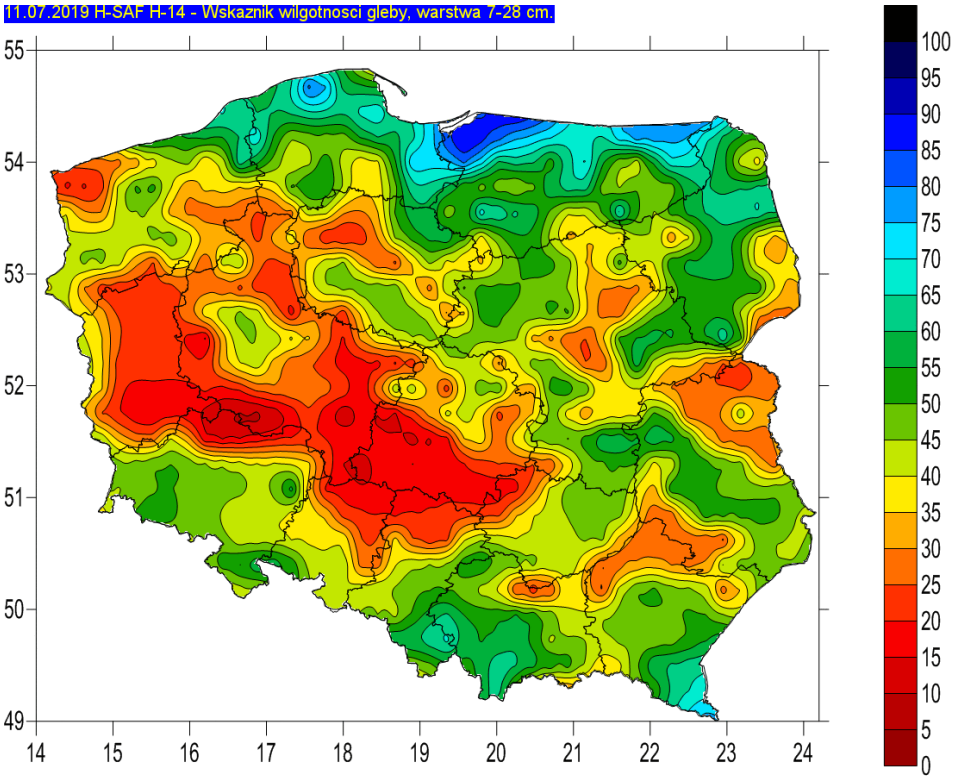

Figure 2. Soil moisture map for layer 7-28cm

The data on soil moisture is useful for hydrological modelling, however without the data on soil texture and SOM content it does not provide the information on soil water deficit, that would allow a reliable decision support on irrigation and prospects for yields.

An indirect measurement of soil moisture in case of soils covered by canopy are being done with thermal images, basin upon various indices related to thermal inertia of canopy cover or temperature/vegetation index method (Petropoulos, 2014; Kishan et al., 2014) (

Table 3).

The models suitable for the estimation of soil humidity basing upon the thermal satellite images can be divided into two groups:

1. Thermal balance models utilizing the effect of stronger warming of areas with water deficit in soil caused by limited real evapo-transpiration (transpiration has cooling effect on the surface);
2. Thermal inertial models basing upon the fact, that wet areas warm up and cool down slower than dry areas, because of the water's large heat capacity, which corresponds to the daily amplitude of temperature being inversely proportional to soil humidity.

For the thermal balance models the starting point of the equations is the thermal balance of the surface of crop cover as a consequence of the energy conservation principle in a time unit. These models can be divided into two categories differing in the representation of surface as one- or two-layer models (Petropoulos, 2014). In the one-layer models the surface of plant and soil is treated as a single uniform layer. In two-layer models the temperature of soil and plant cover is separated into two surfaces, dependent from each other.

In the one-layer category the most popular models are (Petropoulos 2014): SEBS (Surface Energy Balance System (Su, 2002), SEBAL (Surface Energy Balance Algorithm for Land) (Bastiaanssen et al. 1998) and METRIC (Mapping EvapoTranspiration at high Resolution with Internalized Calibration) (Allen et al. 2007).

In the realm of two-layer models the most widely used models are (Petropoulos, 2014): TSEB - Two Source Energy Balance (Norman et al. 1995, French 2002), ALEXI – Atmosphere-Land EXchange Inverse (Anderson et al. 1997) and DisALEXI – Disaggregated ALEXI (Norman et al. 2003).

A separated group of models related to the thermal balance model but based upon empirical observations are models based upon a cloud of points within a coordinate system of two axes: one is surface temperature (Ts) or its function and second is a vegetation index, e.g. the most frequently used NDVI (Normalized Difference Vegetation Index). Among this group, the most popular models are: triangular model (Ts/NDVI), NDTI (Normalized Difference Temperature Index), SWSI (Crop Water Stress Index) and S-SEBI (Simplified Surface Energy Balance Index (chart of Ts/albedo) (Roerink, 2000).

Thermal inertial models are not that frequently used as thermal balance models. Their application as explanatory models for thermal satellite scenes has one large disadvantage. The models assess the dynamics of temperature change in two-time intervals in a single day, e.g. day and night, which is very hard to achieve in existing satellite systems, which have either frequent reacquisition time and low resolution or high resolution and long return time (Petropoulos 2014).

As the combination of high spatial and temporal resolutions is in practice not possible to achieve in a single thermal satellite product an algorithm of combining scenes of high spatial and low temporal resolutions with ones with high temporal and low spatial resolutions can be used to achieve a moderate time and spatial resolution dataset (

Table 3). The refining algorithm bases upon comparative analyses with:

- archive and current precise scenes as reference and correction layers,
- the agricultural-soil map as the reference for spatial variability of soils' hydrological features
- current low spatial resolution but frequent scenes.

Table 3. Sources of free satellite images in thermal band

Satellite	Sensor	Spectral resolution Number of TIR bands, wavelengths	Spatial resolution [m]	Temporal resolution [days]
Terra	ASTER	5 (8,5-11,6 μm)	90	16 on demand
Terra, Aqua	MODIS	16 (3,7-14,4 μm)	1000	2 (day and night) automatic
Landsat 8	TIRS	1 (10,3-12,5μm)	100	16 automatic
Landsat 7	ETM+	1 (10,4-12,2μm)	60 (od 31.05.2013 partially corrupted – 22% of a scene)	
NOAA	AVHRR/3	2/3 (3,5-12,5 μm)	4000	2 (day and night)
ENVISAT	AATSR	3 (3,7-12 μm)	1000	2 (day and night)
Meteosat 8, 9, 10	SEVIRI	8 (3,5-14,4 μm)	3000	0,01
SENTINEL 3a and 3B	SLSTR	9 (0,55-12 μm)	1000	<1

3.2.2 Soil texture

Soil texture is a classification unit depending on the particle size distribution of the soil. There are many classification systems for grain size, however one of the most commonly used is the USDA system in which 12 textures have been separated. The highest number of large particles with diameters above 0.05 mm (sand fraction) contains sand texture and the finest particles with diameters below 0.002 mm (clay fraction) clay texture.

Based on the literature review (Table in annex), it can be formulated that remote sensing of soil textures is based on three groups of methods:

- direct:
    - sand fraction consists mainly of silicon oxide, the bond of which has an absorption band in TIR (about 9000 nm) (Mulder et al. 2011)
    - clay fraction consists of hydrated minerals with numerous hydroxy OH^- groups whose bonds have a characteristic absorption band in SWIR (at 2200 nm) (Chabrillat et al., 2002)
    - clay fraction consists of significant levels of iron oxides with high VIS green light absorption caused by red colour of clays (Ben-Dor 2002),
    - clay fraction in some regions has higher levels of radioactive ^{40}K, ^{232}Th or ^{238}U which can be detected by gamma-ray spectrometers
- indirect based on soil - plant cover interactions

  - on sandy soils with low retention capacity, water stress of plants occurs more often, which results in reduced evapotranspiration and stronger surface heating (detection in the TIR range)
  - long-lasting stress results in reduction of the leaf surface and in extreme case of drying them (NDVI detection)
- indirect based on soil moisture dynamics models (bare soils)
  - clay soils have higher water retention capacity and after uniform rain events are drying longer (detection in the visible range due to water absorption bands, TIR or radar range)
  - clay soils have higher water retention capacity and soil moisture and for that reason they heat up and cool down more slowly (detection in TIR range using images from day and night – thermal inertia methods)

Commonly reported validation results are relatively good, explaining from 30 to 90% clay fraction content variability in the optical range, from 60 to 90% in radar range and about 30% in TIR range. Unfortunately, only in one remote sensing publication the easily available large-scale soil database LUCAS (Tóth et al. 2013), covering entire Europe, was used. Due to the large diversity of the results of remote sensing of soil textures, it seems necessary to make greater use of large publicly available soil databases. Basing studies on such databases is not only cheaper but also allows for easy verification of published results by other researchers.

3.2.3 Typology

No universal direct methods have been found in literature. Indirect methods for soil typology supported with LIDAR are used in numerous studies. (Li et al., 2016). Remote sensing – aerial and satellite, are used however to delineate soil habitat borders and hence provide a valuable information on planning soil sampling campaigns (Kolay, 2009). Some soil types can be easily linked with spectral characteristics e.g. leptosols formed from highly contrasting calcareous rock.

3.2.4 Crop residue content

Crop residue content on upper soil horizon and on its surface depends on tillage practices. Practices that leave more than 30% of crop residue are considered as conservation tillage while other as non-conservation tillage (CTIC, 2002). Conservation tillage practices include: no-till (zero-till and strip-till), ridge till and mulch till, while non-conservation tillage covers reduced till (15-30% residue left on field) and conventional-till, leaving less than 15% crop residue.

The amount of crop residue left on soil surface strongly influences the ratios of SOM stock built-up and hence the soil fertility, overall quality, water retention and soils' resilience to chemical and mechanical degradation (Beare et al., 1994).

Crop residue (non-photosynthetic vegetation) and soils have similar spectra, but crop residue has a unique absorption feature near 2100 nm associated with cellulose and lignin (Daughtry et al., 2005). A review by Zheng et al (2014) presents comparison of several indices used for crop residue assessments based on optical sensors (Table 4) as well as radar sources.

Table 4. Summary of satellite optical remote sensing of crop residue cover and tillage practices (Zheng et al., 2014)

Sensor	Tillage indices	Formula	Description	References
AVIRIS Hyperion	CAI	100 x[0.5(R2030 + R2210) - R2100]	R2030 and R2210 are the reflectances of the shoulders at 2030 nm and 2210 nm, R2100 is at the centre of the absorption. R2>0,77	Daughtry et al. (2006)
ASTER	LCA	100(2 xB6 - B5 -B8)	B5, B6, B7, B8: ASTER shortwave infrared bands 5, 6, 7, and 8	Daughtry et al. (2005)
	SINDRI	(B6 - B7)/(B6 + B7)		Serbin et al. (2009)
LANDSAT TM and ETM+	STI	B5/B7	B2, B4, B5, B7: Landsat bands 2, 4, 5, and 7	van Deventer et al. (1997)
	NDTI	(B5 -B7)/(B5 + B7)		
	Modified Crop Residue Cover	(B5 - B2)/(B5 + B2)		Sullivan et al. (2006)
	NDI5; NDI7	(B4 -B5)/(B4 + B5); (B4 -B7)/(B4 + B7)		McNairn and Protz (1993)
ALI	NDTI	(B5 -B7)/(B5 + B7)	B5 and B7	Galloza et al. (2013)
MODIS				none

Whereas optical systems basically convey information about biological properties of crop residue, SAR imagery conveys information about the physical structure of crop residue, the soil surface, and its moisture status. (Zhang et al., 2014). Although the potential of SAR for soil residue mapping is high, the field conditions shaping the SAR reflectance have high spatial and temporal variability under normal agricultural operating conditions and care must be taken in extrapolating results from controlled experiments onto wider landscape scales (McNairn et al., 2001; Zheng et al., 2014)

3.2.5 Soil Organic Matter

Soil organic matter (SOM) affects soil spectra due to specific vibrations of chemical bonds in parts of organic matter molecules (N-H, O-H, and C-H). In the VIS range, absorption bands responsible for the colour of the soil are associated with vibrations. In the NIR range, absorption bands are mainly associated with OH groups (Angelopoulou et al. 2019).

These properties are successfully used in laboratory and field spectral studies of soils. Unfortunately, due to the impact of soil composition and humidity, there are no universal algorithms for detection of the content of SOM. In case of remote sensing, the situation is exacerbated by plant cover of soil and the impact of the atmosphere.

The analysis of publications on this subject (Table in annex) indicates that there exist three most important groups of remote sensing methods, mainly using the optical range:

- model based, with the assumption on equilibrium of soil respiration and soil organic carbon deposition, using spectral data for assessing amount of vegetation,
- regression models (MLR, PLSR, MARS), using spectral data to build simple models,
- geostatistical methods (cokriging, regression kriging, artificial neural network-simple kriging), using spectral data as co-variables to improve measurement interpolations.

Conclusions of the recent review of progress on SOM remote sensing (Angelopoulou et al. 2019) state that there is a strong need for further integration of remote and proximal SOM analysis methods. This task, however, seems very ambitious, among others due to the poorly developed theoretical basis of soil spectroscopy. Also, the hitherto effects of transfer of proximal detection methods are weak and satisfactory effects presented in some publications usually concern analyses performed with a small number of validation points (most of them with n<100) and in a small area. This observation seems worrisome due to the existence of easily available large-scale soil databases containing SOM information such as the LUCAS database (Tóth et al. 2013) for the EU or the World Soil Information Service (WoSIS) database for the world (Batjes et al 2017). The results of the only analysis carried out on part of LUCAS database samples (n = 713) have shown (Castaldi et al. 2016) that using available bands allow to explain only about 16% and 20% of SOM variability in the case of use the Landsat8 OLI and Sentinel-2 MSI sensors, respectively and 42% of SOM variability when laboratory collected spectra were used. Other weaknesses of remote sensing of SOM, raised in literature, include the lack of an appropriate reference model allowing to assess how much SOM remote sensing results are better than the simplest interpolation or even simple allocation of average SOM content typical for soils that are distinguished on soil maps in a given region and even typical for land use types.

3.5.6 Soil fertility

Nutrient levels in soil remain critically important for achieving high crop yields. Spatial recognition of the content of micro- and macro- elements remains a core of precision agriculture, that aims at minimizing use of production means, like water, fertilizer and pesticides serving the purpose of both increasing farmers' incomes as well as lowering the burden agriculture causes to the environment, producing a healthier food with less traces of chemicals.

At the level of large area satellite estimates of soil fertility, the hitherto usability is limited to delineation of soil habitats, that are used as a basis for further soil sampling (Kishan et al., 2014) using either physical sampling, EC-sampling or proximal spectrophotometry (Debaene et al., 2014) as standard methods used in precision agriculture (Srinivasan (ed.), 2006).

3.5.7 The maturity of Earth Observation techniques in measuring soil properties

The highest maturity of satellite remote sensing has been achieved in estimating soil moisture and crop residue content (Table 5, Table 6, Figure 3. Number of publications in SCOPUS search for EO in estimating soil characteristics3), where indices are derived directly from reflectance data within chosen satellite spectral bands from scenes with bare soil. Methods are promising but existing SAR sensors have too small spatial resolution to be effectively applied in decision support.

The limiting factor of direct reflectance interpretation is that soil remains bare in a limited time within the growing season, hence its temporal resolution is limited. Indirect measurement on the other hand base upon indices derived from the condition of crop cover – either thermal or VNIR.

Table 5. The maturity of EO satellite methods used in estimates of soil properties

Soil Feature	Direct measurement	Indirect indices	Modelling inputs from EO
Moisture	1	1	1
Texture	2	2	1
Type (order)	3	2	2
Crop residue content	1	2	-
SOC	3	2	2
Fertility	3	1	1

1 – EO used widely with numerous publications and on-line services.
2 – EO used but methods are not developed enough to be universal
3 – EO rarely used in case studies, no universal methods present

Table 6. The maturity of aerial methods used in estimates of soil properties

Soil Feature	Direct measurement	Indirect indices	Modelling inputs from EO
Moisture	1	1	1
Texture	2	2	1
Type (order)	3	2	2
Crop residue content	1	2	-
SOC	3	2	2
Fertility	3*	1	1

*Very successful products based upon proximal hyperspectral sensors on the market (farm equipment) and excellent research results (Debaene et al., 2014)

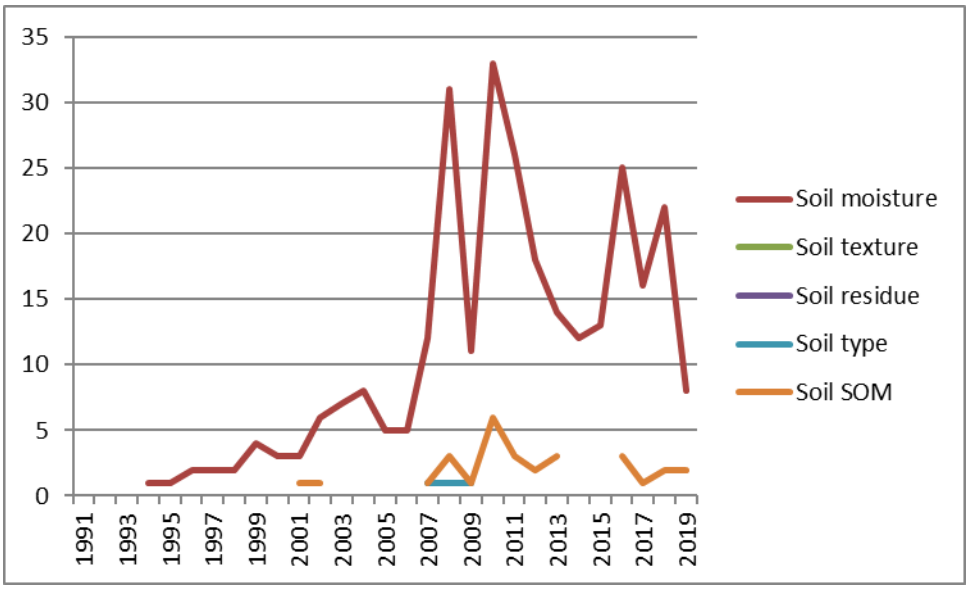

Figure 3. Number of publications in SCOPUS search for EO in estimating soil characteristics

3.2 Potential of the techniques to detect soil degradation processes

Progress on application or Earth Observation methods for detection of selected soil degradation processes is described in this section.

3.2.1 Erosion

Soil erosion has been identified as the most significant soil degradation factor worldwide (Eswaran et al., 2001), creating severe environmental impact and high economic cost on agricultural production and water quality. Pimentel et al. (1995) estimated the total on- and off-site costs of damages by wind and water erosion and the cost of erosion prevention each year at the level of 44,4 billion US$ in the USA alone. Authors estimated that during the last 40 years, nearly one-third of the world's arable land has been lost by erosion and continues to be lost at a rate of more than 10 million hectares per year.

The Joint Research Centre (JRC) of the European Commission's data points at soil erosion as being the most frequent soil degradation process in Europe, estimating its spatial extent to 17% of Europe, from which 8% is assigned to wind erosion (Panagos and Borelli, 2017).The mean soil loss rate in the European Union's erosion-prone lands (agricultural, forests and semi-natural areas) was found to be 2.46 t ha-1 yr-1, resulting in a total soil loss of 970 Mt annually; equal to an area the size of Berlin at 1 metre deep. Policy interventions (i.e. reduced tillage, crop residues, grass margins, cover crops, stone walls and contouring) in the EU such as the Common Agricultural Policy and Soil Thematic Strategy have served to introduce measures to decrease erosion during the last decade by around 9%. However, a lot has to be done as soil erosion rates are higher by a factor of 1.6 compared to soil formation rates (Panagos and Borelli, 2017).

Remote sensing is widely used to detect directly soil erosion or its consequences in the landscape. It is also being used to delineate factors affecting erosion risk and intensity ratios, like topography, canopy cover density etc.

A review by Vrieling (2006) indicated 57 papers addressing detection of soil erosion features and areas affected by means of remote sensing (optical and radar scenes) plus numerous studies utilizing indices of topography (10 papers), soil features and moisture (37), vegetation (55), conservation practices and tillage (13) typically used in USLE model estimates of soil erosion by water (Wischmeier and Smith, 1978).

Direct measurement of erosion ratios and land forms are possible with LIDAR data and methods are well developed and widely used.

Soil erosion remains the most important soil degrading factor, limiting yields and causing land to degrade to the level that becomes unsuitable for land production. Existing methods are well developed but frequent monitoring of soil loss world-wide, semantically and technically coherent, should be put in place for better policy making and cooperation on UN level.

3.2.2 Sealing

Soil sealing by impermeable surfaces related to buildings and transport infrastructure irreversibly limits almost all soil functions. Remote sensing of soil sealing refers either to the direct detection of artificial surfaces in the field of visible radiation or to the detection of the increase in surface temperature caused by blocked evapotranspiration from the soil in thermal infrared bands (TIR). The main dataset of soil sealing for EU, based on long term NDVI observation is the High Resolution Layer Imperviousness (EEA, 2018), available with a resolution of 20m for years: 2006, 2009, 2012 and 2015.

3.2.3 Soil contamination

There is data reported in the literature that spectral methods can be productive for predicting soil contamination with persistent contaminants (Siebielec et al., 2004; Liu et al., 2018; Cheng et al., 2019). However, mainly laboratory or field scanning of soil within infrared or mid-infrared region have given satisfactory results, often at the level of R^2>0.9 between measured and predicted values for some trace metals. The laboratory predictions work better than remote sensing due to weaker effects of various types of noises. Both for laboratory and remote sensing approaches it can be assumed that predictions of contaminant content in soil are based on relationships between soil spectra and soil properties, affecting the contaminant level in soil. For example, soils with greater clay content can accumulate more metals in the topsoil. Therefore, remote spectral predictions of soil contamination with metals might be based on spatial distribution of clay in soil, rather than direct relationships between reflectance values and metals contents. This might lead to the conclusion that detecting spatial distribution of metals in contaminated soils or detecting hot spots requires local or regional statistical models between remote sensing data and metal levels in soil measured using classical laboratory protocols. Regarding the selection of sensors, Shi et al. (2018) suggest that application of multiple proximal/remote-sensed sensors may promote the horizontal and vertical mapping of soil heavy metals. Moreover, combining the satellite and unmanned aerial vehicle-based hyperspectral imaging systems would facilitate technologies that can monitor soil environment more rapidly and accurately at a large scale.

3.2.4 Soil organic carbon decline

Soil organic carbon (SOC) decline is commonly the expected result of climate warming and increase of microbial processes speed (including SOC decomposition) with temperature growth. The practical importance of organic carbon in agricultural soils is related to its beneficial effects on soil structure, increasing soil aeration, buffering capacity in the case of temporary deficiencies of plants nutrients (mainly nitrogen) and to a lesser extent increasing the water retention capacity (Minasny and McBratney 2018).

Remote sensing of SOC changes is almost the same as the detection of the level of SOC, therefore is not be discussed again in this section.

3.2.5 Biodiversity decline

Biodiversity is key to ecosystem resilience to external, including human induced, degrading drivers. Soil biodiversity gains increasing attention in the light of current intensive agricultural practices. Recent study of potential soil biodiversity threats issued by JRC (Orgiazzi et al., 2015) revealed that in 14 out of the 27 considered countries more than 40% of the soils are under moderate-high to high potential risk for all three components of soil biodiversity: soil microorganisms, soil fauna and biological functions. The majority of soils at risk are outside the boundaries of protected areas.

There were no direct EO methods dedicated to soil biodiversity status or decline found in scientific literature, however indirect measurements of landscape diversity and landscape features on which certain species depend, that are being used in assessing aboveground biodiversity can be applied for soil fauna (Chust et al., 2003)

3.2.6 Compaction

Soil compaction is an increase in the soil density caused by pressure, most often from the wheels of agricultural vehicles. The increase in soil density occurs mainly through the reduction of the macropore volume, which results in a decrease in permeability for water and air, and in extreme cases, makes a layer that inhibits the growth of plant roots. Wet soils with high clay fraction content are especially susceptible to excessive compaction.

Since the excessive compaction is mainly the problem of subsurface soil layers, there are no papers focused on direct detecting of soil compaction by remote sensing methods. Remote sensing could be used for assessment of the most important compaction drivers, like clay content and soil moisture but there is still need for some additional research to assess past soil tillage conditions due to soil compaction memory effect (Alaoui and Diserens, 2018).

3.2.7 Floods and landslides

Floods are overflows of water courses by their typical boundaries or excessive accumulation of water in areas not normally covered by water. Landslides are movement of rocks and soil down a slope. Floods and landslides are complex phenomena that locally most strongly depend on the terrain shape, land use, soil moisture and soil mechanical properties.

Digital terrain models with high resolution and quality are the most important for the proper determination of the range of floodplains, as well as areas with a large slope on which there is a risk of landslides. Although remote methods are used to create numerical terrain models, the discussion of related issues goes well beyond the scope of this report.

Reduction of plant cover, especially deforestation on areas with highly inclined slopes, increase landslide risk by reduction of ground surface binding by roots and also increase floods risk by decreased surface roughness for water surface flow and decreased rainfall interception capacity. For this reason, remote sensing of soil vegetation cover and land use is crucial.

On the other hand, the mechanical properties of soils like angle of repose or infiltration rate, important from the point of view of the landslide hazard or floods respectively, are closely related to soil texture. Detection methods of this soil parameter are discussed in chapter 3.1 of this report.

Because of the complexity, most of the data about floods or landslides risk are based on models using partly remote sensing inputs, like Lisflood model in the European Flood Awareness System EFAS (Arnal et al. 2019) or the European landslide susceptibility map ELSUS (Wilde et al. 2018) respectively. In case of landslides there are also direct, fully based on remote sensing radar data, interferometric detection method, implemented in SqueeSAR service (Raspini et al. 2018).

3.2.8 Salinization

Salinity affects the soil in dry and sub-humid climates and is forced by the predominance of evapotranspiration over rainfall. Under such conditions, the dissolved salts from the deeper layers are transported due to capillary actions and accumulate in the soil. Plants show some tolerance to soil salinity. When the threshold value is exceeded, a further salinity increase results in approximately linear yield decrease. In the EU for the purpose of designating subsidized Areas facing Natural Constraints for agriculture (ANC), saline soils are defined as those for which the salinity (measured by electrical conductivity) is greater than or equal to 4 dS m^{-1}.

For detection of salinized soils mainly optical and microwave radiation ranges are used. In optical region specific are absorption bands of gypsum and water in hydrated evaporite minerals. The microwave range detection is based on influence of salts on dielectric constant of soil. Remote detection of salinized soils is still limited mainly to soils with high salt concentration in surface layer (Mulder et al., 2011). Numerous works (e.g. Ávila Aceves et al., 2019), however, demonstrate the local usefulness such simple tools like a normalized difference salinity index NDSI equal to the famous NDVI with a minus sign, which means that in the practice of salinity detection, it is often enough to find a lack of vegetation.

3.2.9 Desertification

A review by Albalawi and Kumar (2013) indicates 11 studies utilizing remote sensing to assess desertification dynamics with indices linked mainly to land cover, sometimes combined with meteorological data. Most often vegetation indices used are NDVI, EVI, SAVI, WDVI and MSAVI. In China remote sensing is utilized in monitoring large area desertification (Zhang and Huisingh, 2018) as a part of national desertification combating system. Due to the homogeneity and wide spatial coverage satellite scenes are a convenient source used for global assessments. Hellden and Tottrup (2008) conveyed such study on desertification utilizing global NDVI data derived from NOAA AVHRR with a resolution of 8km which is suitable for general comparisons at regional scale, but not detailed enough for actual local monitoring and decision support.

3.2.10 The maturity of Earth Observation techniques in measuring soil threats

Nine main soil degradation causes were evaluated in terms of how often remote sensing was used as a method of assessing their intensity and spatial extents (table 7 and 8, figure 4). The most mature remote sensing methods were used in assessments of soil desertification and sealing as well as flooding and landslide occurrence. Some relatively well-developed methods are used in assessments of soil erosion, especially aerial remote sensing. The least developed methods are in assessing SOC decline and biodiversity as well as salinization. Biodiversity is crucial for sustaining soil health, hence the developments in methodologies for these particular studies are most welcome, similarly for SOC.

Table 7. The maturity of EO satellite methods used in estimates of soil degradation

Soil Feature	Direct measurement	Indirect indices	Modelling inputs from EO
Erosion	2	1	1
Sealing	1	-	-
Contamination	3	2	1
SOC decline	-	2	2
Biodiversity decline	3	2	1
Compaction	-	3	3
Floods and landslides	1	-	-
Salinization	3	2	-
Desertification	1	1	1

1 – EO used widely with numerous publications and on-line services.
2 – EO used but methods are not developed enough to be universal
3 – EO rarely used in case studies, no universal methods present

Table 8. The maturity of aerial methods used in estimates of soil degradation

Soil Feature	Direct measurement	Indirect indices	Modelling inputs from EO
Erosion	1	1	1
Sealing	1	-	-
Contamination	2	2	1
SOC decline	-	2	2
Biodiversity decline	3	2	1
Compaction	-	3	3
Floods and landslides	1	-	-
Salinization	3	2	-
Desertification	1	1	1

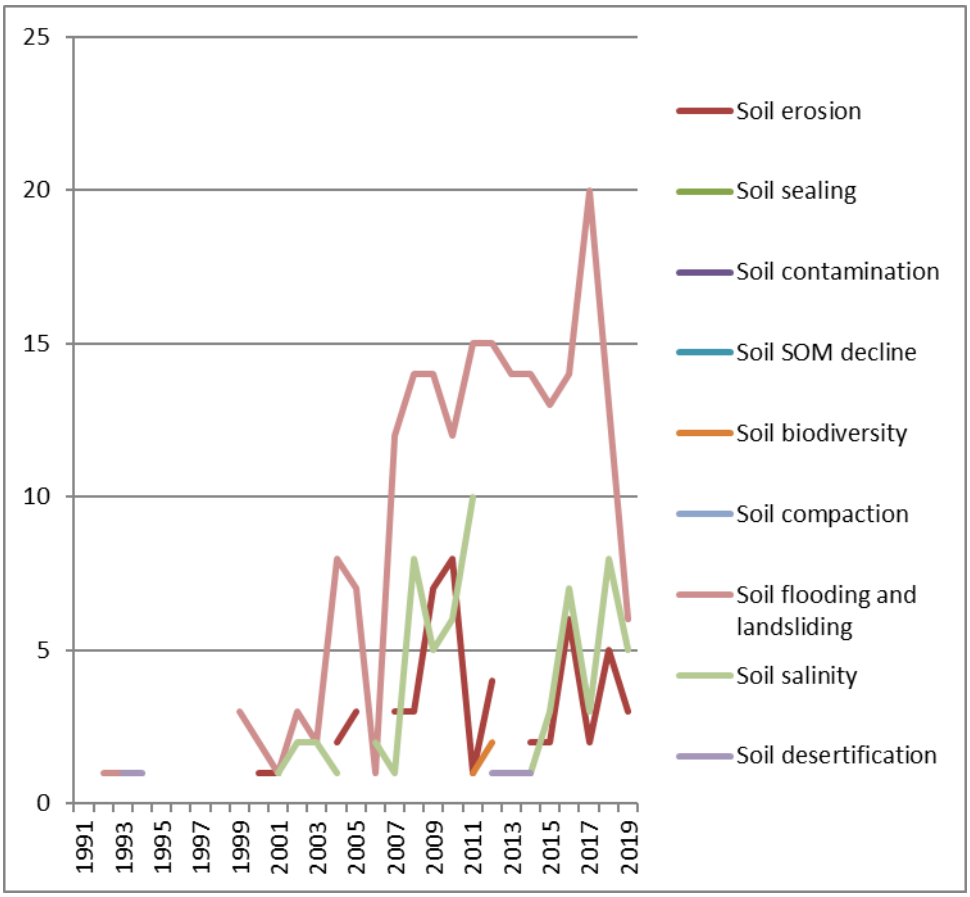

Figure 4. Number of articles in SCOPUS search for EO in soil degradation

4. Practical examples

This chapter elaborates some initiatives and projects that link EO to soil issues.

4.1 European EO programmes and related initiatives

The European Space agency (ESA) has dedicated its resources to observing Earth since the beginning of its first satellite launch in 1977 (Meteosat). Earth observation programmes are encompassed within ESA's Living Planet Programme, that consist of 2 different programmes:

- Earth Observation Envelope Programme (EOEP);
- Earth Watch Programme.

The EOEP remains a core of ESA Earth Observation Strategy 2040 and its 3 main objectives:

- Observe: develop and provide observations to better understand the complexity of our planet and monitor its health;
- Understand: enable improved predictions of the physical interaction of society with the earth system;
- Decide: inform decision makers and citizens on scenarios and consequences of political and economic decisions regarding our planet.

The Earth Watch Programme on the other hand is designed as continuous deliverer of Earth observation data for use in operational services and consists of the following components:

- the Meteosat Third Generation (MTG)
- the Global Monitoring for Environment and Security (GMES) Space Component (GSC)
- the Climate Change Initiative (GMECV+)
- the InCubed programme
- the ALTIUS mission
- the Proba-V exploitation.

COPERNICUS

From the point of view of agricultural and environmental services, the most important and actually most successful component is GMES. It turned into the European COPERNICUS programme, supported with well-designed access services and preparatory work, disseminating the COPERNICUS possibilities within the society and industry. The GMES, now COPERNICUS, space component under ESA responsibility comprises satellites called Sentinels and instrumentations. The Sentinels carry a range of technologies, such as radar and multi-spectral imaging instruments for land, ocean and atmospheric monitoring:

- Sentinel-1 provides all-weather, day and night radar imagery for land and ocean services;
- Sentinel-2 provides high-resolution optical imagery for land services;
- Sentinel-3 provides high-accuracy optical, radar and altimetry data for marine and land services;

- Sentinel-4 and Sentinel-5 will be instruments carried on the next generation of meteorological satellites, namely Meteosat Third Generation (MTG) and MetOp Second Generation, providing data for atmospheric composition monitoring from geostationary orbit and polar orbit, respectively;
- Sentinel-5 Precursor will bridge the gap between Envisat (Sciamachy data in particular) and Sentinel-5;
- Sentinel-6 will provide radar altimetry data to measure global sea-surface height, primarily for operational oceanography and for climate studies

COPERNICUS, as the European Earth monitoring system, consists of a complex set of systems which collect data from multiple sources: earth observation satellites and in situ sensors such as ground stations, airborne sensors, and sea-borne sensors. It processes this data and provides users with reliable and up-to-date information through a set of services related to environmental and security issues[5].

The services address six thematic areas: land, marine, atmosphere, climate change, emergency management, and security. They support a wide range of applications, including environment protection, management of urban areas, regional and local planning, agriculture, forestry, fisheries, health, transport, climate change, sustainable development, civil protection, and tourism.

INSPIRE

The INSPIRE Directive entered into force in May 2007. It establishes an infrastructure for spatial information in Europe to support Community environmental policies, and policies or activities which may have an impact on the environment[6].

INSPIRE is based on the infrastructures for spatial information established and operated by the 28 Member States of the European Union. The Directive addresses 34 spatial data themes needed for environmental applications, with key components specified through technical implementing rules[6].

The INSPIRE Directive laid down the foundations of an interoperable, harmonized spatial information infrastructure system for the EU. The components of INSPIRE (metadata, data models and services) ease the practical use of spatial datasets in multi-national context. Three out of four INSPIRE Directive's Annex 2 spatial data themes correspond to COPERNICUS programme; they are elevation, land cover and orthoimagery. Annex 1 themes build a spatial foundation and spatial reference for the whole infrastructure: reference systems, grid definitions, geographical names, administrative units etc. Annex 3 themes supplement the first two annexes with less critical themes, yet often utilized in environmental reporting and assessments addressing soil, CAP and land cover issues. The common use of established data models, services based upon open standards and metadata describing both allows truly interoperable infrastructure for spatial data and information in the EU.

[5] www.copernicus.eu
[6] www.inspire.ec.europea.eu

4.2 Precision farming

Precision agriculture is an information-based farming system with high degree of integration of monitoring and selective or variable rate application of water, fertilizer and pesticide products, aimed at increasing the farm revenue by limiting the use of production means to gain a similar level of yield from a farmer's perspective on one hand and putting less pressure on natural resources, climate and quality of the environment from the perspective of public health. The more precise use of pesticides, fertilizers and water as basic production means is achieved via recognition of spatial diversity of soil cover and temporal changes in growing conditions. Both aspects are realised extensively with remote sensing.

Remote sensing has a wide range of uses in precision farming, including:

- zoning fields for varying application rates of fertilizers and water;
- adjusting fertilization to soil fertility or crop condition;
- detecting diseases;
- observing changes in plant cover over time;
- estimating crop yields;
- identifying pest and weed coverage;
- assessing the impacts of severe weather events and animal damage.

Remote Sensing techniques also play an important role in assessing crop condition and yield forecasting, acreage estimates of specific crops, detection of crop pests and diseases, disaster location and mapping, wild life management, water supply information and management, weather forecasting, rangeland management, and livestock surveys (Liaghat and Balasundram, 2010).

Most of the satellite remote sensing applications in precision farming on bare soil are dealing with zoning of the fields for later applications, based upon the variation of reflectance in various bands corresponding to different values of SOC and moisture content. Other remote sensing methods base upon reflectance of different wavelengths by plant cover e.g. NDVI. The resolution of freely available products reach 10m (Sentinel 3) while proprietary scenes e.g. from SPOT satellite reach 1,5m (panchromatic) and 6m (multispectral). The prediction of soil properties with high quality and resolution have been done with proximal sensing with sensors installed on tractors since early 1990's in real-time sensing of soil spatial variation of SOC and soil moisture. Further development in this technology by Christy (2008) allowed simultaneous measurement of soil organic matter content, soil moisture, soil pH, soil carbon and soil phosphorus, potassium, and calcium. Since 90' farming machines are being equipped with on the go sensors for yield estimation, plant vigour (NDVI), soil EC etc.

Satellite and aerial remote sensing in precision farming became a standard tool for land zoning, monitoring crop conditions and estimating water stress, however the available satellite scenes were not detailed enough for smaller plots. With the revolution in drone technology, that caused a rapid growth of investments in smart farming in 2016, the industry followed with optical sensing products dedicated to small unmanned aerial vehicles, like small light multispectral sensors NIR + VIS.

Additionally, the implementation of machine learning and AI in drone steering software made land surveying easy enough for complete newbies, while still the extraction of information form image data remains a specialist work. However, these tasks are also being automated and put as on-line tools. It is expected that image recognition and new spectral sensors will revolutionize smart farming and allow much faster implementation of completely autonomous agricultural machinery and farm management systems.

One of the most recent technologies released for high quality measurements usable in precision farming are proximal spectral sensors, used at ground level to estimate current soil fertility and conditions. Research with hyperspectral sensors of high resolution (5nm) revealed high predictability of soil features in certain wavelength ranges: texture, soil moisture, NPK, and SOM, reaching r^2=0,6-0,96 for the latter. These bands have a high practical potential, but often cannot be applied into satellite missions because of the absorption of particular wavelengths by the earth's atmosphere but still they can be utilized in new spectral imaging products for aerial or proximal sensing. One of the pioneering initiatives in this domain is EnMap[7] - the Environmental Mapping and Analysis Program (EnMAP), which is a German hyperspectral satellite mission that aims at monitoring and characterising the Earth's environment on a global scale. Another driver for innovation in satellite remote sensing is the progress in nano-satellite builds and lower prices of putting nanosatellites on the earth's orbit.

4.3 Experiments or projects that link EO and soil information

LUCAS land use and soil database - The LUCAS project is mainly focused on land use and land cover monitoring in thousands of control areas deployed across the EU, for every third year since 2006. From about 20 thousands of monitoring points, soil samples have been already taken. For all samples the following data have been released: main soil fractions, SOC, total N, extractable P and K, carbonates and soil pH value (Tóth et al. 2013).

WoSIS (World Soil Information Service) soil profile database – containing 96 000 georeferenced soil profiles data from the whole world (Batjes et a. 2017). Most of them have information on main fractions as well as SOC and soil pH.

All **long-term experiments** across Europe (for example the project "Advancing Earth Observation Application in Agriculture" at the famous Rothamsted station[8]) are potential data sources and sites for method testing. Long term experiments provide physical measurement, so that remotely sensed data can be calibrated to increase the quality of correlation between reflectance in certain wavelengths and particular soil properties. They are also crucial in machine learning, including AI, that needs real-life data to learn on how to interpret spectral response to change in soil condition.

[7] www.enmap.org
[8] https://www.rothamsted.ac.uk/projects/advancing-earth-observation-applications-agriculture-developing-wall-wall-data-products

4.4 International Earth Observation initiatives

NASA Earth Observing System (EOS) is a coordinated series of polar-orbiting satellites for long-term global observations of Earth systems. EOS released numerous satellite missions, including: Landsat 7 and 8, Terra, GRACE, and many more. The website of Project's Science Office is to be found here https://eospso.nasa.gov/.

GEO Group on Earth Observations is a partnership consisting of more than 100 national governments creating a global network connecting governments, researchers, data providers, businesses and general public to address global challenges with EO tools and methods. The GEO community (http://earthobservations.org) is creating a Global Earth Observation System of Systems (GEOSS), integrating observing systems and granting access to many EO sources via GEOO portal at: https://geoportal.org.

BigData UN Global Working Group's Satellite Imagery and Geo-Spatial Data Task Team (https://unstats.un.org/bigdata/taskteams/satellite/) is aiming at providing a strategic vision of a global work plan towards utilizing Earth Observation and geo-spatial data for assessing post-2015 development goals.

UNOSAT: UNITAR's Operational Satellite Applications Programme – a programme delivering imagery analysis to relief and development organizations (https://www.unitar.org/unosat/).

GLOSIS – Global Soil Information System, an initiative within **Global Soil Partnership**, aiming at making soil data from around the globe available. GLOSOLAN - Global Soil Laboratory Network, being a part of GLOSIS, now contains a group addressing spectroscopy of soils.

5. Recommendations on how to improve and to create synergies in the EU

1. A wide interoperability framework, similar to the European Spatial Data Infrastructure (SDI), introduced by INSPIRE Directive (2007/2/EC), should be prepared and issued for soil monitoring from EO. The soil data theme is present in the INSPIRE directive in the least important group of data in Annex 3. The INSPIRE models impose only the information on soil classification in metadata and class value in data, which makes international assessment equally impossible as before. The SDI should address at least: field sampling, laboratory measurements, remote sensing methods, sensor descriptions. It should foster open standards for semantics, data formats, metadata and services;
2. Monitoring programs for soil properties and soil degradation should be organized separately due to different regimes and methodologies both of these aspects have.
3. EU should foster an effective OpenData movement on Earth observation data, meant as: 1) an access point to all the data produced by science on a fair basis with costs reflecting the real cost of producing and sharing the data; 2) a legal framework addressing the rights of data producers/custodians;
4. Soil data samplings and measurements financed by EU should be available with open access;
5. Improve sensor resolution in new satellite missions, especially in thermal band spectrum from currently best 90m to future best 20m. This will allow for a wider recognition of water stress in plant for drought monitoring and, potentially, irrigation advise;
6. Research on hyperspectral imaging in satellite and airborne missions has to be put forward. The EnMAP mission is one of the potential success stories to be put through. This will allow for far more precise soil quality assessments in very fast time, that will have huge effect on practical applications like smart farming as well as monitoring of soil health;
7. Innovations in less expensive hyperspectral sensors for airborne imaging can trigger a wide variety of innovations in soil oriented practical applications, especially precision farming (smart farming), drought management and can play a crucial role in helping to adapt to ongoing climate change. Wider availability of high-quality data results in more case studies relating soil and the environment, hence on long terms it should result in a better understanding on soil-plant-climate relationships;
8. Methods of remote sensing that are mature require further improvement of spatial and temporal scale of data acquisition while methods not yet developed within certain scopes related to soils should be developed in high-risk research grants based upon fundamental research in soil and spectrophotometry. Those grants can have a cascading scheme, starting form 30-40 grants for the level of proof-of-concept through prototyping and testing, ending up with 4-5 grants with most promising sensors or methods to be developed to TRL9;

9. More online services with interoperable, INSPIRE-compliant data exchange standards, should be put in place for companies and public authorities to build their decision support and information services. This will allow enhancing the remote recognition methods with AI and BigData technologies, that will help to improve our understanding of soil environment and hence make better decisions;
10. Use the LUCAS soil database to verify the soil remote sensing to a greater extent. This dataset has a great potential for machine learning and BigData techniques;
11. Well monitored multiannual experiments for research in the field of soil remote sensing (such as Rothamsted, section 4.3) are the critical core for future development of soil monitoring using EO. Long-term soil experiments in various spatial scales and geographical locations should be maintained as part of EU strategic research facilities. Measured data is the key for machine learning both in terms of building algorithms as well as validating them;
12. The soil research community recommends funding several research projects addressing methods of better harmonization of soil data collected with different methods;
13. We recommend widening research aimed at understanding end users (farmers) needs according to better utilization of RS based products;
14. Following FAO's findings on the rates of soil degradation, in light of the upcoming climate crisis and growing human population, global monitoring of soil quality and global action on its preservation is a strategic security issue for human kind. In parallel to high-resolution small-scale technologies, an effort should be made to harmonize all the available remote sensing information globally, providing researchers and decision makers with tools that will allow making good policies for food production as well as assure prediction and reacting to soil related problems.

References

1. Aicha H., Fouad Y., Walter C., Viscarra Rossel R.A., Chabaane Z.L., Sanaa M., 2009. Regional prediction of soil organic carbon content from spectral reflectance measurements. Biosystems Eng., 104: 442-446
2. Alaoui A., Diserens E., 2018. Mapping soil compaction – A review. Current opinion in environmental science & health, 5, 60-66. https://doi.org/10.1016/j.coesh.2018.05.003
3. Albalawi E.K., Kumar L., 2013. Using remote sensing technology to detect, model and map desertification: A review. Journal of Food, Agriculture & Environment Vol.11 (2): 791-797
4. Allen R. G., Tasumi M., Morse A., Trezza R., Wright L., Bastaanssen W., Kramber W., Lorite I. J., Robinson C.W. 2007. Satellite-based energy balance for mapping evapotranspiration with internalized calibration (METRIC) – Applications, J. Irrig. Drain. Eng, 133(4): 395-406
5. Anderson M. C., Norman J. M., Diak G. R., Kustas W.P., 1997. A two-source time Integrated model for estimating surface fluxes for thermal infrared satellite observations, Remote Sens. Environ, 60: 195-216
6. Angelopoulou T., Tziolas N., Balafoutis A., Zalidis G., Bochtis D., 2019: Remote Sensing Techniques for Soil Organic Carbon Estimation: A Review. Remote Sens. 2019, 11, 676. https://doi.org/10.3390/rs11060676
7. Arnal l., S.-S. Asp, C. Baugh, A. de Roo, J. Disperati, F. Dottori, R. Garcia, M. Garcia-Padilla, E. Gelati, G. Gomes, M. Kalas, B. Krzeminski, M. Latini, V. Lorini, C. Mazzetti, M. Mikulickova, D. Muraro, C. Prudhomme, A. Rauthe-Schöch, K. Rehfeldt, P. Salamon, C. Schweim, J.O. Skoien, P. Smith, E. Sprokkereef, V. Thiemig, F. Wetterhall, M. Ziese, 2019. EFAS upgrade for the extended model domain – technical documentation, EUR 29323 EN, Publications Office of the European Union, Luxembourg, ISBN 978-92-79-92881-9, doi: 10.2760/806324, JRC111610
8. Ávila Aceves E., Peinado Guevara H.J., Cruz Enriquez A., Campos Gaxiola J.D.J., Pellegrini Cervantes M.D.J., Herrera Barrientos J., Herrera L.E., Peinado Guevara V.M., and Samuel C.L., 2019: Determining Salinity and Ion Soil Using Satellite Image Processing. Polish Journal of Environmental Studies, 28(3), 1549-1560. https://doi.org/10.15244/pjoes/81693
9. Badora D., 2016. Use of the grace model in the assessment of the groundwater level in the context of the availability of water for agriculture in the basin of the Vistula. Polish Journal of Agronomy, 27: 21-31
10. Bastiaanssen W. G. M., Meneti M., Feddes A., Holstag A.A.M. 1998. A remote sensing surface energy balance algorithm for land (SEBAL): 1. Formulation, J. Gydrol., 198-212
11. Batjes N.H., Ribeiro, E. van Oostrum, A. Leenaars J., Hengl T. and de Mendes J., 2017: WoSIS: Providing standardised soil profile data for the world, Earth System Science Data 9, 1-14. https://doi.org/10.5194/essd-9-1-2017
12. Beare, M. H., P. F. Hendrix, et al., 1994. Aggregate-Protected and Unprotected Organic Matter Pools in Conventional- and No-Tillage Soils. Soil Science Society of America Journal 58(3): 787-795.
13. Ben-Dor E., 2002. Quantitative remote sensing of soil properties. Advances in Agronomy. 75. 173-243. https://doi.org/10.1016/S0065-2113(02)75005-0
14. Bhunia G.S., Shit P.K., Pourghasemi H.R., 2017. Soil organic carbon mapping using remote sensing techniques and multivariate regression model, Geocarto International. https://doi.org/10.1080/10106049.2017.1381179
15. Bridges, E.M. I.D. Hannam, L.R. Oldeman, F.W.T. Penning de Vries, S.J. Scherr, S. Sombatpanit (Eds.), Response to Land Degradation, Science Publishers Inc, Enfield, NH, USA (2001), pp. 20-35
16. Brown D.J., Shepherd K.D., Walsh M.G., Deawyne M., Reinsch T.G., 2006. Global soil characterization with VNIR diffuse reflectance spectroscopy. Geoderma, 132: 273-290

17. Castaldi F., Palombo A., Santini F., Pascucci S., Pignatti S., Casa R., 2016. Evaluation of the potential of thecurrent and forthcoming multispectral and hyperspectral imagers to estimate soil texture and organic carbon. Remote Sens. Environ., 179, 54–65. https://doi.org/10.1016/j.rse.2016.03.025
18. Chabrillat S., Goetz A.F.H., Krosley L., Olsen H.W., 2002. Use of hyperspectral images in the identification and mapping of expansive clay soils and the role of spatial resolution. Remote Sens. Environ. 82 (2–3), 431–445. https://doi.org/10.1016/S0034-4257(02)00060-3
19. Cheng H., Shen R., Chen Y., Wan Q., Shi T., Wang J., Wan Y., Hong Y., Li X. 2019. Estimating heavy metal concentrations in suburban soils with reflectance spectroscopy. Geoderma 336: 59-67
20. Christy C.D., 2008. Real-time measurement of soil attributes using on-the-go near infrared reflectance spectroscopy. Computers and Electronics in Agriculture, 61: 10-19
21. Chust G., Pretus J.L., Ducrot D.,Bed`os A., Deharveng I., 2003. Response of Soil Fauna to Landscape Heterogeneity: Determining Optimal Scales for Biodiversity Modelling, Conservation Biology, 17: 1712–1723
22. Connor D., Martin P. G. & Scott T. B., 2016. Airborne radiation mapping: overview and application of current and future aerial systems, International Journal of Remote Sensing, 37:24, 5953-5987, DOI: 10.1080/01431161.2016.1252474
23. CTIC, 2002. National Survey of Conservation Tillage Practices. Conservation Technology Information Center, West Lafayette, IN. , http://www.ctic.purdue.edu/resourcedisplay/322/ (accessed 28.07.13)
24. Daughtry, C.S.T., Doraiswamy, P.C., Hunt Jr., E.R., Stern, A.J., McMurtrey III, J.E., Prueger, J.H., 2006. Remote sensing of crop residue cover and soil tillage intensity. Soil and Tillage Research 91, 101–108.
25. Daughtry, C.S.T., Hunt Jr., E.R., Doraiswamy, P.C., McMurtrey III, J.E., 2005. Remote sensing the spatial distribution of crop residues. Agronomy Journal 97, 864–871.
26. Debaene G., Niedzwiecki J., Pecio A., 2010. Visible and near-infrared spectrophotometer for soil analysis: preliminary results. Polish J., Agr., 3:3-9
27. Debaene G., Niedzwiecki J., Pecio A., Zurek A., 2014. Effect of the number of calibration samples on the prediction of several soil properties at the farm scale. Geoderma 2014-2015: 114-125
28. Dematte J.A.M., Alves M.R., Terra F.S., Bosquilia R.W.D., Fongaro C.T., Barros P.P.S., 2016. Is It Possible to Classify Topsoil Texture Using a Sensor Located 800 km Away from the Surface? Rev Bras Cienc Solo;40: e0150335. http://dx.doi.org/10.1590/18069657rbcs20150335
29. Dematte J.A.M., Guimaraes C.C.B., Fongaro C.T., Vidoy E.L.F., Sayao V.M., Dotto A.C., Santos N.V., 2018. Satellite spectral data on the quantification of soil particle size from different geographic regions. Rev Bras Cienc Solo 42:e0170392. https://doi.org/10.1590/18069657rbcs20170392
30. EEA, 2018. Copernicus Land Monitoring Service – High Resolution Layer Imperviousness: Product Specifications Document, 1-39.
31. Eswaran, H., Lal, R., Reich, P.F., 2001. Land degradation: an overview. In: Bridges, E.M., Hannam, I.D., Oldeman, L.R., Penning de Vries, F.W.T., Scherr, S.J., Sombatpanit, S. (Eds.), Response to Land Degradation. Science Publishers Inc, Enfield, NH, USA, pp. 20 – 35
32. Fidencio P.H., Poppi R.J., De Andrade J.C., 2002. Determinaiton of organic matter in soils uysing radial basis function networks and near infrared spectroscopy. Anal. Chim. Acta., 453: 125-134
33. French A. T., Schmugge T., Kustas W. P., 2002. Estimating evapotranspiration over El_reno,Oklahoma with ASTER imagery, Agronomie, 22:105-106

34. Galloza, M.S., Crawford, M.M., Heathman, G.C., 2013. Crop residue modeling and mapping using Landsat, ALI, Hyperion and airborne remote sensing data. IEEE Journal of Selected Topics in Applied Earth Observations and Remote Sensing 6: 446–456
35. Gomez C., Viscarra R.A., Mcbratney A.B., 2008. Soil organic carbon prediction by hyperspectral remote sensing and field vis-NIR spectroscopy: An Australian case study. Geoderma, 146, 403–411. https://doi.org/10.1016/j.geoderma.2008.06.011
36. Gorrab A., Zribi M., Baghdadi N., Mougenot B., Fanise P., Chabaane Z.L., 2015: Retrieval of Both Soil Moisture and Texture Using TerraSAR-X Images. Remote Sens., 7, 10098-10116. https://doi.org/10.3390/rs70810098
37. Hellden, U., Tottrup, C., 2008 Regional desertification: A global synthesis. Global Planet. Change, 64, 169–176.
38. Jones H. G., Vaughan R. A., 2010. Remote sensing of vegetation – Principles, techniques, and applications, Oxford University Press, 353 p.
39. Kishan G., Kumar S., Saha s. K., PAtek N.R., 2014. Remote Sensing in Soil Fertility Evaluation and Management. In book: Bioresources for Sustainable Plant Nutrient Management Chapter: 19 Publisher: Serial Publishing House, New DelhiEditors: Ramesh Chandra and K.P. Raverkar: 509-533
40. Kolay A.K., 2009. Remote Sensing and Assessment of Soil Resources. Atlantic Pub.& Distr. Ltd., pp" 493.
41. Li Z., Catry T., Dessay N., Roux E., Seyler F., 2016. Mapping soil typologies using geomorphologic features extracted from DEM and SAR data: A environmental factor affecting malaria transmission in the Amazon. IGARSS 2016 - 2016 IEEE International Geoscience and Remote Sensing Symposium, Jul 2016, Beijing, China.
42. Liaghat S., Balasundram S.K., 2010. A Review: The Role of Remote Sensing in Precision Agriculture. American Journal of Agricultural and Biological Sciences 5 (1): 50-55
43. Liao K., S. Xu, J. Wu, Q. Zhu, 2013. Spatial estimation of surface soil texture using remote sensing data, Soil Science and Plant Nutrition, 59:4, 488-500. https://doi.org/10.1080/00380768.2013.802643
44. Liu J., Zhang Y., Wang H., Du Y. 2018. Study on the prediction of soil heavy metal elements content based on visible near-infrared spectroscopy. Spectrochimica Acta - Part A: Molecular and Biomolecular Spectroscopy 199: 43-49
45. Martin P.G., Moore J., Fardoulis J.S., Payton O.D., 2016: Radiological Assessment on Interest Areas on the Sellafield Nuclear Site via Unmanned Aerial Vehicle, Remote Sens., 8(11), 913. https://doi.org/10.3390/rs8110913
46. McNairn, H., Duguay, C., Boisvert, J., Huffman, E., Brisco, B., 2001. Defining the sensitivity of multi-frequency and multi-polarized radar backscatter to post-harvest crop residue. Canadian Journal of Remote Sensing 27, 247–263
47. McNairn, H., Protz, R., 1993. Mapping corn residue cover on agricultural fields in Oxford County, Ontario, using Thematic Mapper. Canadian Journal of Remote Sensing 19, 152–159
48. Messerschmiedt I., Cuelbas C. J., Poppi R.J., De Andrade J. C., De Arbeu C.A., 1999. Determination of organic matter in soils by FTIR/diffuse refectance multivariate calibration. J. Chemom., 13: 265-273
49. Minasny B., McBratney A.B., 2018. Limited effect of organic matter on soil available water capacity. European Journal of Soil Science, 69, 39–47. https://doi.org/10.1111/ejss.12475
50. Mirzaee S., Ghorbani-Dashtaki S., Mohammadi J., Asadi H., Asadzadeh F., 2016: Spatial variability of soil organic matter using remote sensing data, CATENA, 145, 118-127. https://doi.org/10.1016/j.catena.2016.05.023.
51. Mondal A., Khare D., Kundu S., Mondal S., Mukherjee S., Mukhopadhyay A., 2017. Spatial soil organic carbon (SOC) prediction by regression kriging using remote sensing data, The

Egyptian Journal of Remote Sensing and Space Science 20, 1, 61-70. https://doi.org/10.1016/j.ejrs.2016.06.004.

52. Moros J., Martinez-Sanches M.J., Perez-Sirvent C., GArrigues S., de la Guardia M., 2009. Testing of the Region of Murcia soils by near infrared diffuse reflectance spectroscopy and chemometrics. Talanta, 78: 388-398
53. Mulder V.L., de Bruin S., Schaepman M.E., Mayr T.R., 2011: The use of remote sensing in soil and terrain mapping — A review, Geoderma, 162, 1–2, 1-19. https://doi.org/10.1016/j.geoderma.2010.12.018.
54. Müller B., Bernhardt M., Jackisch C., and Schulz K., 2016: Estimating spatially distributed soil texture using time series of thermal remote sensing – a case study in central Europe, Hydrol. Earth Syst. Sci., 20, 3765-3775. https://doi.org/10.5194/hess-20-3765-2016
55. Nachtergaele F., 2014: Soil salinity, in: JRC, Updated common bio-physical criteria to define natural constraints for agriculture in Europe. Definition and scientific justification for the common criteria; Technical Factsheets, EUR 26638. https://doi.org/10.2788/79958
56. Nawar S., Buddenbaum H., Hil, J., 2015: Digital Mapping of Soil Properties Using Multivariate Statistical Analysis and ASTER Data in an Arid Region. Remote Sens., 7, 1181-1205. https://doi.org/10.3390/rs70201181
57. Niedzwiecki J., Debaene G., 2013. Modern chemometric methods for measuring soil organic matter in soils. Studia I Raporty IUNG-PIB, Z 35(9): 199-212
58. Norman J. M. , Kustas W. P., Humes K.S., 1995. A two-source approach for estimating soil and vegetation energy fluxes in observations of directional radiometric surface temperature. Agric. For Meteorol. 77: 263-293
59. Norman J. M., Anderson M. C., Kustas W. P., French A. N., Mecikalski J., Torn R., Diak G. R. et al., 2003. Remote sensing of surface energy fluxes at 101-m pixel resolutions. Water Resour. Res., 39(8): 1221
60. Orgiazzi A., Panagos P., Yigini Y., Dunbar M.B., Gardi C., Montanarella L., Ballabio C., 2015. A knowledge-based approach to estimating the magnitude and spatial patterns of potential threats to soil biodiversity, Science of The Total Environment, Volumes 545–546: 11-20
61. Panagos P., Borelli P., 2017. Soil erosion in Europe: Current status challenges and future developments. https://ec.europa.eu/jrc/en/publication/soil-erosion-europe-current-status-challenges-and-future-developments
62. Petropoulos G.P., 2014: Remote sensing of Surface Turbulent Energy Fluxes. 49-84, in.: Remote sensing of Energy Fluxes and Soil Moisture Content. Taylor and Francis Group, Boca Raton.
63. Pimentel D., Harvey C., Resosudarmo P., Sinclair K., Kurz D., McNair M., Crist S., Shpritz L., Fitton L., Saffouri R., Blair R., 1995. Environmental and Economic Cost of Soil Erosion and Conservation Benefits. Science 267(5201):1117-23
64. Raspini F., Bianchini S., Ciampalini A., Del Soldato M., Solari L., Novali F., … Casagli N., 2018: Continuous, semi-automatic monitoring of ground deformation using Sentinel-1 satellites. Scientific reports, 8(1), 7253. https://doi.org/10.1038/s41598-018-25369-w
65. Read C.F., Duncan D.H., Ho C.Y.C., White M., Vesk P.A., 2017: Useful surrogates of soil texture for plant ecologists from airborne gamma-ray detection. Ecol Evol.;8:1974–1983. https://doi.org/10.1002/ece3.3417
66. Roerink G., Su Z., Meneti M., 2000. S0SEBI: A simple remote sensing algorithm to estimate the surface energy balance. Phys. Chem. Earth, Part B, 25(2): 147-157
67. Sayl K. N., Afan H. A., Muhammad N. S., and ElShafie A., 2017: Development of a Spatial Hydrologic Soil Map Using Spectral Reflectance Band Recognition and a Multiple-Output Artificial Neural Network Model, Hydrol. Earth Syst. Sci. Discuss. https://doi.org/10.5194/hess-2017-13

68. Selige T., Böhner J., and Schmidhalter U., 2006. High resolution topsoil mapping using hyperspectral image and field data in multivariate regression modeling procedures, Geoderma, vol.136, issue.1-2, pp.235-244. https://doi.org/10.1016/j.geoderma.2006.03.050
69. Serbin, G., Hunt Jr., E.R., Daughtry, C.S.T., McCarty, G.W., Doraiswamy, P.C., 2009. An improved ASTER index for remote sensing of crop residue. Remote Sensing 1: 971–991
70. Shi T., Guo L., Chen Y., Wang W., Shi Z., Li Q., Wu G. 2018. Proximal and remote sensing techniques for mapping of soil contamination with heavy metals. Applied Spectroscopy Reviews 53: 783-805.
71. Siebielec G., McCarty G.W., Stuczynski TI., Reeves III J.B., 2004. Near- and Mid-Infrared Diffuse Reflectance Spectroscopy for Measuring Soil Metal Content. J. Environ. Quality, 33: 2056-2069
72. Singh D., Kathpalia A., 2007: An efficient modeling with GA approach to retrieve soil texture, moisture and roughness from ERS-2 SAR data. Prog. Electromagnetics Res.77, 121–136. https://doi.org/10.2528/PIER07071803
73. Souza J.J., Ferreira F.J.F., Rocha H.O., Mantovani L.E., 1997. Application of Airborne Gamma Ray Spectroscopy and Remote Sensing to Map Contamination by Fertilizers, In: 5th International Congress of the Brasilian Geophysical Society, 1997, Sao Paulo. Expanded Abstracts. Rio de Janeiro: Sociedade Brasileira de Geofísica. v. 2.851-853.
74. Srinivasan A. (Ed.), 2006. Handbook of Precision Agriculture. Principles and Applications. Food Products Press, pp: 657
75. Su Z., 2002. The Surface Energy Balance System (SEBS) for estimation of turbulent heat fluxes. Hydrol. Earth Syst. Sci., 6(1): 85-89
76. Sullivan, D.G., Truman, C.C., Schomberg, H.H., Endale, D.M., Strickland, T.C., 2006. Evaluating techniques for determining tillage regime in the Southeastern Coastal Plain and Piedmont. Agronomy Journal 98 (5) 1236–1246
77. Tóth G., Jones A., Montanarella L. (eds.), 2013. LUCAS Topsoil Survey: methodology, data and results, Luxembourg: Publications Office of the European Union, EUR26102EN Scientific and Technical Research series, pp141. https://doi.org/10.2788/97922
78. van Deventer, A.P., Ward, A.D., Gowda, P.H., Lyon, J.G., 1997. Using Thematic Mapper data to identify contrasting soil plains and tillage practices. Photogrammetric Engineering & Remote Sensing 63, 87–93.
79. Vather T., Everson C., Mengistu M., Franz T., 2018. Cosmic ray neutrons provide an innovative technique for estimating intermediate scale soil moisture. S Afr J Sci. 2018;114(7/8), Art. #2017-0422, 9 pages. http://dx.doi.org/10.17159/sajs.2018/20170422
80. Vaudour E., Gomez C., Fouad Y., Lagacherie P., 2019. Sentinel-2 image capacities to predict common topsoil properties of temperate and Mediterranean agroecosystems. Remote Sens. Environ., 223, 21–33. https://doi.org/10.1016/j.rse.2019.01.006
81. Vinci A., Brigante R., Todisco F., Mannocchi F., Radicioni F., 2015. Measuring rill erosion by laser scanning, CATENA, Volume 124: 97-108
82. Viscarra Rossek R., 2007. Robust modelling of soil diffuse reflectance spectra by “bagging-PLSR”, J. Near Infrared Specrtosc., 15: 39-47
83. Viscarra Rossel R.A., Minasny B., Roudier P., McBratney A.B., 2006. Colour space models for soil science. Geoderma 133 (3–4), 320–337. https://doi.org/10.1016/j.geoderma.2005.07.017
84. Vrieling A., 2006. Satellite remote sensing for water erosion assessment: A review. Catena 65 (2006): 2 – 18
85. Wang D-C., Zhang G-L., Zhao M-S., Pan X.Z., Zhao Y-G., Li D-C., Macmillan B., 2015. Retrieval and Mapping of Soil Texture Based on Land Surface Diurnal Temperature Range Data from MODIS. PLoS ONE 10(6): e0129977. https://doi:10.1371/journal.pone.0129977

86. Wang L., Qu J., J, 2009. Satellite remote sensing applications for surface soil moisture monitoring: A review. Front. Earth Sci. China 2009, 3(2): 237–247
87. Wawer R., Nowocien E., Podolski B., 2013a. Sediment uptake rates under extreme rainfall in controlled conditions. Journal of Food Agriculture and Environment, Vol.11 (1): 1089-1093
88. Wawer R., Nowocien E., Podolski B., 2013b. Wind erosion rates for ten soils under threshold wind speed in controlled conditions. Journal of Food Agriculture and Environment, vol. 11(2): 1432-1436
89. Wetterlind J., Stenberg B., Soderstrom M., 2010. Increased sample point density in farm soil mapping by local calibration ofvisible and near infrared prediction models. Geoderma, 156: 152-160
90. Wilde M., Günther A., Reichenbach P., Malet J.-P., Hervás J., 2018. Pan-European landslide susceptibility mapping: ELSUS Version 2, Journal of Maps, 14:2, 97-104, https://doi.org/10.1080/17445647.2018.1432511
91. Wischmeier, W.H., Smith, D.D., 1978. Predicting rainfall-erosion losses: a guide to conservation planning. Agricultural Handbook, vol. 537. U.S. Department of Agriculture
92. Zhang Z., Huisingh D., 2018. Combating desertification in China: Monitoring, control, management and revegetation. Journal of Cleaner Production, Volume 182: 765-775
93. Zheng B., Campbell J. B., Serbin G., Galbraith J. M., 2014. Remote sensing of crop residue and tillage practices: Present capabilities and future prospects. Review. Soil & Tillage Research 138 (2014): 26–34
94. Zhou T., Shi P., Luo J., Shao Z., 2008. Estimation of soil organic carbon based on remote sensing and process model, Front. For. China, 3: 139. https://doi.org/10.1007/s11461-008-0038-3
95. Zribi M., Kotti F., Lili-Chabaane Z., Baghdadi N., BenIssa N., et al. 2012. Soil texture estimation over a semi-arid area using TerraSAR-X radar data. IEEE Geoscience and Remote Sensing Letters, 2012, 9(3), 353-357. http://hal.ird.fr/ird-00679652

ANNEX I Detailed literature review results

Table A1. Summary of the available publications about remote sensing of soil texture.

Method description	validation period	validation area	validation results for clay fraction Cl%	additional limitations	reference
Landsat 7 optical bands 1) bare soil mask: NDVI = (B4 - B3)/(B4 + B3)<0.25 vegetation elimination, IVI = (B5 - B7)/(B5 + B7)<0.15 crop residue elimination; 2) multiple linear regression for bare soils - bands 5 and 7 most significant (difference in reflectance intensity due to low levels of iron oxides in sandy soils)	1999-2011; June-October	Brazil; 5 000 km^2	Cl_{pred} = 0.201*Cl_{meas}+ 4.19 n=729 R^2 = 0.63 RMSE = 27	-	Demattê et al. 2018
airborne gamma-ray spectrometry of ^{40}K and ^{232}Th - clay was positively related to radiometric counts; boosted regression tree (BRT) models	not relevant	Australia; 40 000 km^2	n=398 predictive performance ~30%	extrapolation possibilities restricted to regions where sediments have the same origins	Read et al. 2017
Landsat 8 optical bands - 6, 1, 7 most significant; artificial neural network model	2014 August	Iraq; 13 370 km^2	(only calibration) n=25 R^2 = 0.73 RMSE=3.5	small number of samples, no validation	Sayl et al. 2017
ASTER instrument of the TERRA satellite – 90m thermal band no. 13; PCA used for extraction of PCs within TIR time series; multiple linear regression for relation soils texture to PCs	January 2001 - June 2012; snow and cloud free images	Luxembourg, 288 km^2	R^2 = 0.35 (calibration) n=212 RMSE=7.2 (cross- validation)	small study area	Müller et al. 2016

Method description	validation period	validation area	validation results for clay fraction Cl%	additional limitations	reference
MODIS sensor TIR band – 1km land surface diurnal temperature range (DTR) product; linear regression between clay and DTR for bare soil	2007 November	China; 5130 km^2	n~30 R^2 ~ 0.30 RMSE ~ 5.0	method requires similar starting soil moisture conditions (e.g. after homogeneous rainfall event), small number of samples	Wang et al. 2015
Landsat 5 optical bands; bare soil supervised texture classification using the Gaussian Maximum Likelihood algorithm	2002-2007 August-September	Brazil; 350 km^2	n=200 R^2 ~ 0.90	quality of supervised classification depends on classifier experience - how selected training sites are representative for the range of spectral variability found within a particular soil class (influenced by actual vegetation or terrain moisture distribution); small study area	Dematte et al. 2016
Landsat 7 optical bands – only no. 7 (SWIR) significant; Comparison of three methods for bare soils (NDVI<0.1): a) linear regression b) kriging c) cokriging	2007 November	China; 3166 km^2	n=58 a) R^2 = 0.36 (calibration) b) R^2 = 0.06 RMSE=5.6 (crossvalidation) c) R^2 = 0.28 RMSE=4.7 (crossvalidation)	small number of samples, no validation for regression	Liao et al. 2013
TerraSAR-X radar data: X-band 9.65 GHz, incidence angle 35°, HH polarization, 1 m pixel; difference between two radar signals: first day after a heavy rain, second after three weeks dry conditions; regression estimate of exponential relation after linearization	2010 March	Tunisia; ~ 1500 km^2	n=30 R^2 = 0.60 (calibration) RMSE=12.5 (validation)	period between radar images should be short because of roughness changes of vegetation cover, small number of samples	Zribi et al. 2012

Method description	validation period	validation area	validation results for clay fraction Cl%	additional limitations	reference
TerraSAR-X radar data: X-band 9.65 GHz, incidence angle 36°, HH polarization, 1.8 m pixel; linear regression between radar data derived bare soil moisture (NDVI<0.21) and clay	2013 November – 2014 January	Tunisia; ~ 1500 km^2	n=34 R^2 = 0.62 (calibration) RMSE=10.8 (validation)	period between radar images should be short because of roughness changes of vegetation cover, small number of samples	Gorrab et al. 2015
airborne HyMap scanner: 6 m pixel; selected bare soils; 1) partial least-square regression (PLSR) using recorded spectral signature reduced to 5 relevant factors 2) multiple linear regression (MLR) using 4 selected relevant wavelengths: 902, 950, 998 and 1165 nm	1999 May	Germany; ~ 200 km^2	n=60 1) PLSR: R^2 = 0.71 RMSE=4.2 2) MLR: R^2 = 0.65 RMSE=3.8 (calibration, crossvalidation) n=12 2) MLR: R^2 = 0.64 (validation)	small study area, small number of validation samples	Selige et al. 2006
ASTER instrument of the TERRA satellite – optical bands; selected bare and dry soils; 1) multivariate adaptive regression splines (MARS) – 5 basis functions 2) partial least squares regression (PLSR) - 4 latent variables	2006 May	Egypt; 380 km^2	n=86 1) MARS: R^2 = 0.94 RMSE=4.4 2) PLSR: R^2 = 0.90 RMSE=5.6 (crossvalidation)	small study area	Nawar et al. 2015

Method description	validation period	validation area	validation results for clay fraction Cl%	additional limitations	reference
			n=32 1) MARS: R^2 = 0.89 RMSE=6.9 2) PLSR: R^2 = 0.87 RMSE=7.6 (validation)		
ERS-2 SAR radar data: C-band, 5.3 GHz, VV polarization; global optimization by genetic algorithm (GA) for the retrieval of soil parameters and moisture – assumption that soil dielectric constant is linear function of soil fractions	July 2001; March 2004	India; 10 250 km^2	n=27 R^2 = 0.82-0.85 SE=7-8	validation on the same scene as calibration, small number of validation samples	Singh, Kathpalia 2007
Sentinel – 2A, optical range; Partial least-squares regression (PLSR)	2016 March	France; a) 48 km^2 b) 221 km^2	a) n=72 R^2 = 0.39 RMSE=1.23 (cross-validation) b) n=143 R^2 = 0.42 RMSE=56.4 (cross-validation)	small study area	Vaudour et a. 2019

Method description	validation period	validation area	validation results for clay fraction Cl%	additional limitations	reference
Soil data and spectra from databases: A) PONMAC n=163 B) LUCAS n=713 Spectra obtained under laboratory conditions were resampled to simulate satellite imagers in optical range: a) Hyperion b) Landsat 8 OLI c) Sentinel-2 MSI; Partial Least Square Regression (PLSR)	not relevant	Italy cropland area	Aa) R^2=0.58; RMSE=5.9% Ab) R^2=0.43; RMSE=7.0% Ac) R^2=0.61; RMSE=5.7% Ba) R^2=0.61; RMSE=8.0% Bb) R^2=0.38; RMSE=10.1% Bc) R^2=0.40; RMSE=9.9% (multiple jack-knifing validation)	artificial satellite data from laboratory spectral scanning may not reproduce all natural atmospheric conditions	Castaldi et al. 2016

Table A2. Summary of the available publications about remote sensing of SOM

Method description	validation period	validation area	validation results for soil organic carbon C_{org} (g/kg)	additional limitations	reference
airborne HyMap scanner: 6 m pixel; selected bare soils; 1) partial least-square regression (PLSR) using recorded spectral signature reduced to 7 relevant factors 2) multiple linear regression (MLR) using 4 selected relevant wavelengths: 800, 830, 1194 and 1322 nm	1999 May	Germany; ~ 200 km^2	n=60 1) PLSR: R^2 = 0.90 RMSE=0.29 2) MLR: R^2 = 0.86 RMSE=0.22 (calibration, crossvalidation) n=12 2) MLR: R^2 = 0.89	small study area, small number of validation samples	Selige et al. 2006

Method description	validation period	validation area	validation results for soil organic carbon C_{org} (g/kg)	additional limitations	reference
			(validation)		
AVHRR NDVI 8 km, mean monthly product; Soil base respiration in equilibrium state: a=NPP(NDVI) exp(-b*T) / f(P/ET0) NPP and f respectively according to CASA and Century model, linear regression for SOC(a)	not relevant	China whole country	n=17? R^2 = 0.78 (validation)	many assumptions incorporated to NPP and soil respiration models	Zhou et al. 2008
ASTER instrument of the TERRA satellite – optical bands; selected bare and dry soils; 1) multivariate adaptive regression splines (MARS) – 8 basis functions 2) partial least squares regression (PLSR) - 4 latent variables	2006 May	Egypt; 380 km^2	n=86 1) MARS: R^2 = 0.79 RMSE=0.26 2) PLSR: R^2 = 0.73 RMSE=0.3 (crossvalidation) n=32 1) MARS: R^2 = 0.73 RMSE=0.34 2) PLSR: R^2 = 0.71 RMSE=0.36 (validation)	small study area	Nawar et al. 2015

Method description	validation period	validation area	validation results for soil organic carbon C_{org} (g/kg)	additional limitations	reference
Landsat 4-5; SOM analysed on different land uses (forest, paddy fields, fallows, sandy areas); 1) Linear regression between SOC and NDVI 2) Linear regression between SOC and Bare Soil Index BSI = 100 + 100(B3 - B1)/(B5 + B3 - B4 - B1) 3) Multiple linear regression SOC(NDVI, BSI)	2013 June	India; 324 km^2	n=50 1) SOC = 0.161 + 0.029NDVI R^2 = 0.54 2) SOC = 10.11 - 0.04*BSI R^2 = 0.51 3) SOC = 4.26 + 11.91NDVI - 0.02BSI R^2 = 0.71 (calibration)	small study area; small number of validation samples relative to land use differentiation	Bhunia et al. 2017
Landsat TM; Aster; visible and thermal bands; Regression kriging with predictor variables: NDVI, Brightness Index BI, Greenness Index GI, Wetness Index WI, Vegetation Temperature Condition Index VTCI, elevation, slope, Compound Topographic Index CTI	?	India; 20 558 km^2	n=147 RMSE=0.23 (calibration) n=63 RMSE=0.28 (validation)	-	Mondal et al. 2017
Hyperion hyperspectral sensor 400–2500 nm (152 bands), pixel 30m; Partial least-squares regression (PLSR)	2006 October, December	Australia; 16.2 km^2	n=72 R^2 = 0.51 RMSE=0.73 (cross-validation)	small study area	Gomez et al. 2008
Landsat 7, optical range; artificial neural network-simple kriging (ANNSK)	2014 July, August	Azerbaijan; 410 km^2	n=100 R^2 = 0.63 RMSE=0.27 (calibration)	-	Mirzaee et al. 2016

Method description	validation period	validation area	validation results for soil organic carbon C_{org} (g/kg)	additional limitations	reference
Sentinel – 2A, optical range; Partial least-squares regression (PLSR)	2016 March	France; a) 48 km^2 b) 221 km^2	a) n=72 R^2 = 0.56 RMSE=1.23 (cross-validation) b) n=104 R^2 = 0.02 RMSE=3.71 (cross-validation)	small study area	Vaudour et al. 2019
Soil data and spectra from databases: A) PONMAC n=166 B) LUCAS n=713 Spectra obtained under laboratory conditions were resampled to simulate satellite imagers in optical range: a) Hyperion b) Landsat 8 OLI c) Sentinel-2 MSI; Partial Least Square Regression (PLSR)	not relevant	Italy cropland area	Aa) R^2=0.62; RMSE=0.22% Ab) R^2=0.50;RMSE=0.25% Ac) R^2=0.56; RMSE=0.23% Ba) R^2=0.27; RMSE=0.46% Bb) R^2=0.16; RMSE=0.51% Bc) R^2=0.20; RMSE=0.50% (multiple jack-knifing validation)	artificial satellite data from laboratory spectral scanning may not reproduce all natural atmospheric conditions	Castaldi et al. 2016